
Reports

11-1978

Hydrography and hydrodynamics of Virginia estuaries. XVII, Mathematical ecosystem modeling study of the York River

P. V. Hyer

Virginia Institute of Marine Science

A. Y. Kuo

Virginia Institute of Marine Science

C. S. Fang

Virginia Institute of Marine Science

W. J. Hargis Jr.

Virginia Institute of Marine Science

Follow this and additional works at: <https://scholarworks.wm.edu/reports>

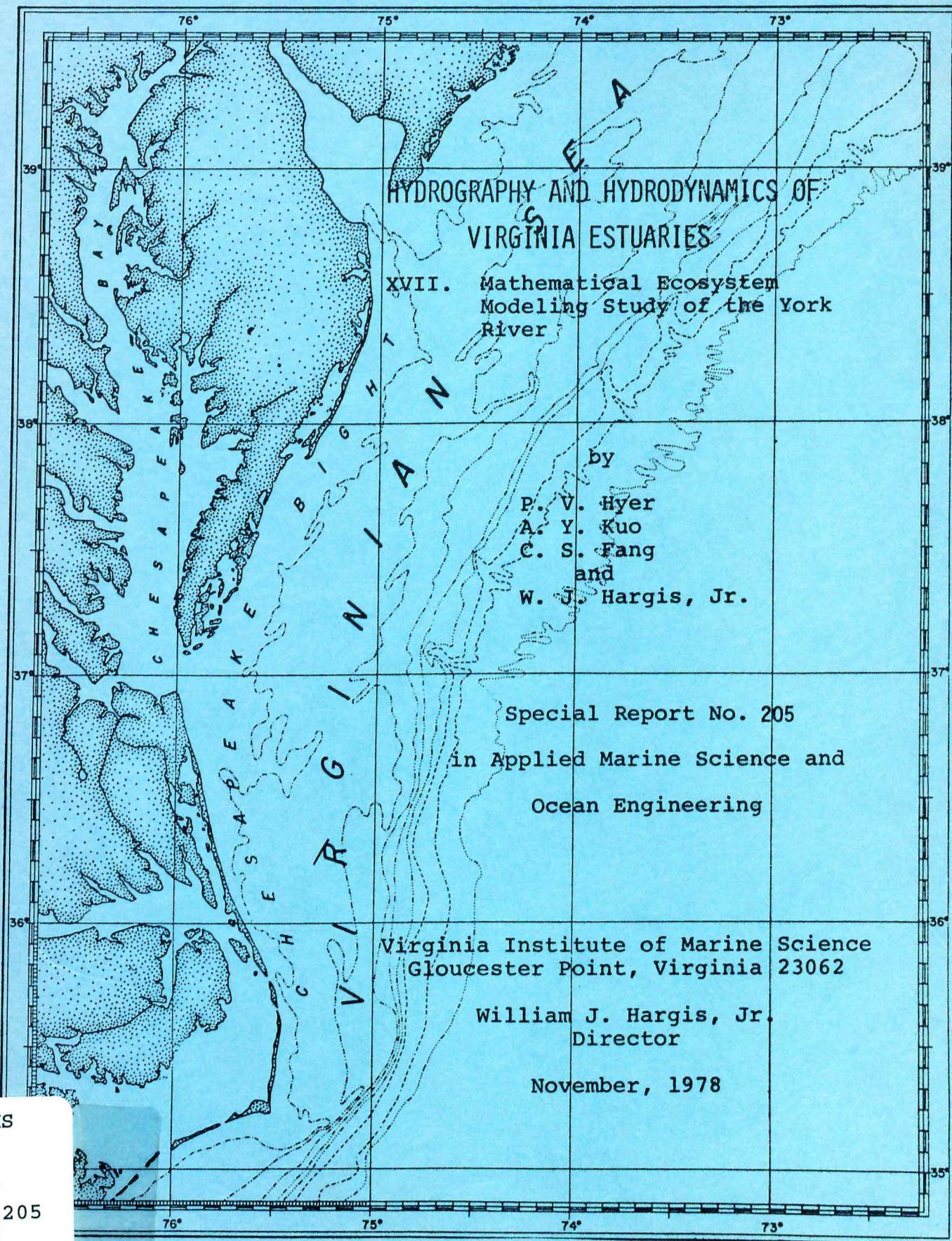


Part of the [Marine Biology Commons](#), and the [Oceanography Commons](#)

Recommended Citation

Hyer, P. V., Kuo, A. Y., Fang, C. S., & Hargis, W. J. (1978) Hydrography and hydrodynamics of Virginia estuaries. XVII, Mathematical ecosystem modeling study of the York River. Special Report in Applied Marine Science and Ocean Engineering; No. 205. Virginia Institute of Marine Science, College of William and Mary. <http://dx.doi.org/doi:10.21220/m2-epac-mw64>

This Report is brought to you for free and open access by W&M ScholarWorks. It has been accepted for inclusion in Reports by an authorized administrator of W&M ScholarWorks. For more information, please contact scholarworks@wm.edu.



HYDROGRAPHY AND HYDRODYNAMICS OF
VIRGINIA ESTUARIES

XVII. Mathematical Ecosystem
Modeling Study of the York
River

by

P. V. Hyer
A. Y. Kuo
C. S. Fang
and
W. J. Hargis, Jr.

Special Report No. 205
in Applied Marine Science and
Ocean Engineering

Virginia Institute of Marine Science
Gloucester Point, Virginia 23062

William J. Hargis, Jr.
Director

November, 1978

VIMS
GC
1
S67
no.205
c.2

HYDROGRAPHY AND HYDRODYNAMICS OF VIRGINIA ESTUARIES

XVII. Mathematical Ecosystem Modeling
Study of the York River

by

P. V. Hyer
A. Y. Kuo
C. S. Fang
and
W. J. Hargis, Jr.

PREPARED UNDER
THE COOPERATIVE STATE AGENCIES PROGRAM
OF
THE VIRGINIA STATE WATER CONTROL BOARD
AND THE
VIRGINIA INSTITUTE OF MARINE SCIENCE

Project Officers

Dale Jones
Michael Bellanca

Special Report No. 205
in Applied Marine Science and
Ocean Engineering

Virginia Institute of Marine Science
Gloucester Point, Virginia 23062

William J. Hargis, Jr.
Director

November, 1978

VIMS
GC
1
E67
no. 205
0.2

TABLE OF CONTENTS

	Page
List of Figures.....	iii
List of Tables.....	v
Acknowledgements.....	vi
Abstract.....	vii
I. Summary and Conclusions.....	1
II. Introduction.....	4
III. Description of Study Area.....	6
IV. Description of the Water Quality Model.....	12
V. Model Calibration and Verification.....	34
References.....	71
Appendix A. User's Manual for Quasi-Three Dimensional Ecosystem Model.....	73

LIST OF FIGURES

Figure		Page
1	Downstream sub-basin of York drainage basin.....	7
2	York and Pamunkey time of slack water relative to York River.....	9
3	York River calculated tidal prism.....	11
4	Flow diagram for ecosystem model.....	13
5	Exploded view of model segment showing numbering scheme for compartments.....	20
6	Bottom demand sampling locations and model segmentation.....	30
7	York River salinity calibration results.....	36
8	York River organic nitrogen calibration results.....	37
9	York River ammonia nitrogen calibration results.....	38
10	York River nitrate plus nitrite calibration results.	39
11	York River organic phosphorus calibration results...	40
12	York River inorganic phosphorus calibration results.	41
13	York River chlorophyll 'a' calibration results.....	42
14	York River carbonaceous BOD calibration results.....	43
15	York River dissolved oxygen calibration results.....	44
16	York River fecal coliform calibration results.....	45
17	York River salinity verification.....	47
18	York River organic nitrogen verification.....	48
19	York River ammonia nitrogen verification.....	49
20	York River nitrate plus nitrite verification.....	50
21	York River organic phosphorus verification.....	51
22	York River inorganic phosphorus verification.....	52

LIST OF FIGURES (Cont'd)

Figure		Page
23	York River chlorophyll 'a' verification.....	53
24	York River carbonaceous BOD verification.....	54
25	York River dissolved oxygen verification.....	55
26	Sensitivity of CBOD to magnitude of point sources...	57
27	Sensitivity of salinity to dispersion coefficient...	58
28	Sensitivity of salinity to estuarine circulation parameter.....	59
29	Sensitivity of salinity to fresh-water inflow.....	61
30	Sensitivity of salinity to downstream boundary condition.....	62
31	Sensitivity of CBOD to decay rate.....	63
32	Sensitivity of ammonia to nitrification rate.....	64
33	Sensitivity of nitrate plus nitrite to nitrifi- cation rate.....	65
34	Sensitivity of coliform concentration to variations in bacterial decay rate.....	66

LIST OF TABLES

Table		Page
1	Flow Records for Beulahville and Hanover, Virginia, 1976.....	25
2	Benthic Oxygen Demand Studies, York River, 1976....	29
3	Point Sources of Loading Used in Calibration and Verification.....	46

ACKNOWLEDGEMENTS

We thank the Virginia Water Control Board for its continuing support of this project.

The comments and criticisms of Dr. Wen Kao of the Bureau of Water Control Management are greatly appreciated.

We thank the Hampton Roads Water Quality Agency for providing some of the point source discharge data used in the calibration and verification.

We thank Ms. Shirley Crossley for her patient typing of this report.

ABSTRACT

The York River drainage basin is rural, with an economy based on farming, logging, fishing and recreation. Water quality conditions are generally good, with low chlorophyll and nutrients and low fecal coliform counts. Dissolved oxygen concentrations are high except for periodic deoxygenation of the water deeper than 8 m in the reach extending 10 km upstream of the mouth.

A quasi-three dimensional tidal average model was constructed and calibrated using intensive field data collected in June and July, 1976 and verified using slack water run data from September, 1976. The model components are: salinity, fecal coliform, chlorophyll, CBOD, dissolved oxygen, organic nitrogen, ammonia, nitrate plus nitrite, organic phosphorus and inorganic phosphorus.

Model runs revealed that the deep-water deoxygenation is a natural condition little influenced by human activity and that the York is insensitive to point source loadings, owing to its enormous volume.

I. SUMMARY AND CONCLUSIONS

1. This report concerns the calibration and verification of an ecosystem model for the York River between the mouth and Terrapin Point, about 30 miles (4-8 km) upstream, and the underlying theory and approximations.
2. The York drainage basin is relatively unpopulated and agricultural in nature. Industries include pulp and paper processing, oil refining and fossil-fuel power generation. Recreational water uses are important. The region is characterized by a hot summer, relatively dry fall and mild, wet winter.
3. A hydrographic survey was conducted in June and July, 1976 at eight transects in the York plus the mouths of the Mattaponi and Pamunkey. Time series data on salinity, temperature, dissolved oxygen, CBOD, chlorophyll, organic nitrogen, ammonia, nitrate, nitrite, total phosphorus and soluble reactive phosphorus were collected. There were three stations per transect in the York and one station each at the mouths of the Mattaponi and Pamunkey.
4. The midstream stations were sampled for the same variables in slack water runs in September, 1976.

5. In the vicinity of West Point, individual dissolved oxygen measurements were found to be as low as 4.5 mg/l, but the daily average was found to be above 5.0 mg/l.
6. Between Gloucester Point and the mouth of the York, the river is quite deep, approaching 20 m in places. Data from the summer of 1976 and other data reveal an oxygen depletion zone in the deeper layers. Daily average dissolved oxygen in this region was below three mg/l, with some individual measurements below one mg/l.
7. Chlorophyll concentration was below ten micrograms per liter in almost all cases. Chlorophyll growth appears to be primarily light-inhibited, i.e. turbidity limited. Nitrogen availability appears to be a second inhibiting factor.
8. Nutrient concentrations are insufficient to support a bloom condition.
9. Fecal coliform counts rarely exceed 3.6 MPN/100 ml.
10. Salinity at the downstream boundary ranged from 20 to 23 ppt. Temperature throughout the estuary ranged from 24°C to 26°C, marking this period of time as less than critical from the standpoint of water quality.

11. The low dissolved oxygen in the deeper layers off Yorktown seems to be a naturally occurring condition little influenced by human activities.

12. The enormous water volume of the York makes it insensitive to the magnitude of point discharges typically present.

II. INTRODUCTION

The first substantial water quality investigation of the York River was known as "Operation York River", carried out in October, 1969. This project concentrated on the Mattaponi and Pamunkey Rivers, but included a portion of the York near West Point. The product was a tidal-time model of salinity, dissolved oxygen and biochemical oxygen demand (hereafter abbreviated BOD) (Hyer, et al., 1971). This model was used by the Division of Water Resources for a study of point source waste discharges in the vicinity of West Point. In 1969 there was also another oxygen balance and dye tracer study of the confluence of the Mattaponi and Pamunkey Rivers (Harrison & Fang, 1971).

Tidal currents and bathymetry were measured in 1970 for VEPCO as part of a study to determine the environmental effects of a proposed expansion of the fossil-fueled power plant at Yorktown. This same construction project became the occasion for an ecological study from 1972 to 1974 (Jordan, et al., 1975). Frequent slack water runs were made in the summer of 1972 to study the aftermath of Hurricane Agnes (Hyer & Ruzecki, 1974).

In 1973, the entire York estuary was studied intensively. Measurements included both water quality and tidal current from the mouth to the confluence of the Mattaponi and Pamunkey. The data collected were used for a tidal-time water quality model of salinity, dissolved oxygen and BOD (Hyer, et al., 1975). This model was also successfully applied. This model was

one-dimensional, i.e., averaged over cross-section. However, the lower part of the York River is deeper than ten meters for most of its length and in places approaches thirty meters. Thus, in the summer when water temperatures exceed 20°C , dissolved oxygen stratification occurs even though tidal current amplitude is greater than 1 ft/sec (0.3 m/sec). Data reported by Jordan (1975) show the normally occurring summertime dissolved oxygen difference between surface and twenty meters to be five mg/l to seven mg/l or greater. Hence, the deeper waters frequently fell below three mg/l of dissolved oxygen. This dissolved oxygen stratification has been observed with varying degrees of salinity stratification from two parts per thousand to six parts per thousand.

In view of this dissolved oxygen stratification, a two-layer model was needed for the York River. Furthermore, the width of this estuary (up to two nautical miles or 3.7 km) indicated the use of lateral segmentation. The model to be used has three lateral compartments in each of two layers, or six compartments per longitudinal reach. Hence, it is called a quasi-three-dimensional model.

This model only deals with tidal average conditions of observed quantities and with mean flows. The biochemical interaction processes are identical to those used for the Small Coastal Basin models (Hyer, et al., 1977).

III. DESCRIPTION OF STUDY AREA

The tidal portion of the York River watershed has remained relatively rural, with a heavy dependence on farming (chiefly corn and soybeans) and logging. Commercial fishing of oysters, crabs and pelagic fish is also important. Industry is concentrated at both ends of the York. Upstream, at West Point, (see Figure 1) is a pulp and kraft paper mill. Downstream, near the mouth, are an oil refinery and a fossil-fueled electric power plant.

The climate is humid-subtropical. There are approximately 45 inches of rain, of which approximately 12 inches is runoff. Precipitation is lowest between September and January and highest in July and August. Owing to evapotranspiration, however, the heavy thunderstorms of summer have much less effect on fluvial flow than do the rains of spring. Air temperature in January varies from a low of approximately 30°F (-1°C) to a high of 50°F (10°C). In July the mean daily maximum temperature is approximately 88°F (30°C) and the minimum is 68°F (20°C).

The most representative stream gauging stations in the drainage basin are at Hanover (drainage area 1081 mi² or 2800 km²), on the Pamunkey and Beulahville (drainage area 601 mi² or 1557 km²) on the Mattaponi. The average discharges at these stations are 963 cfs (27.3 m³sec⁻¹) and 580 cfs (16.4 m³sec⁻¹) respectively. The total drainage area of the York River Basin is 2540 mi² or 6580 km². River discharge tends to

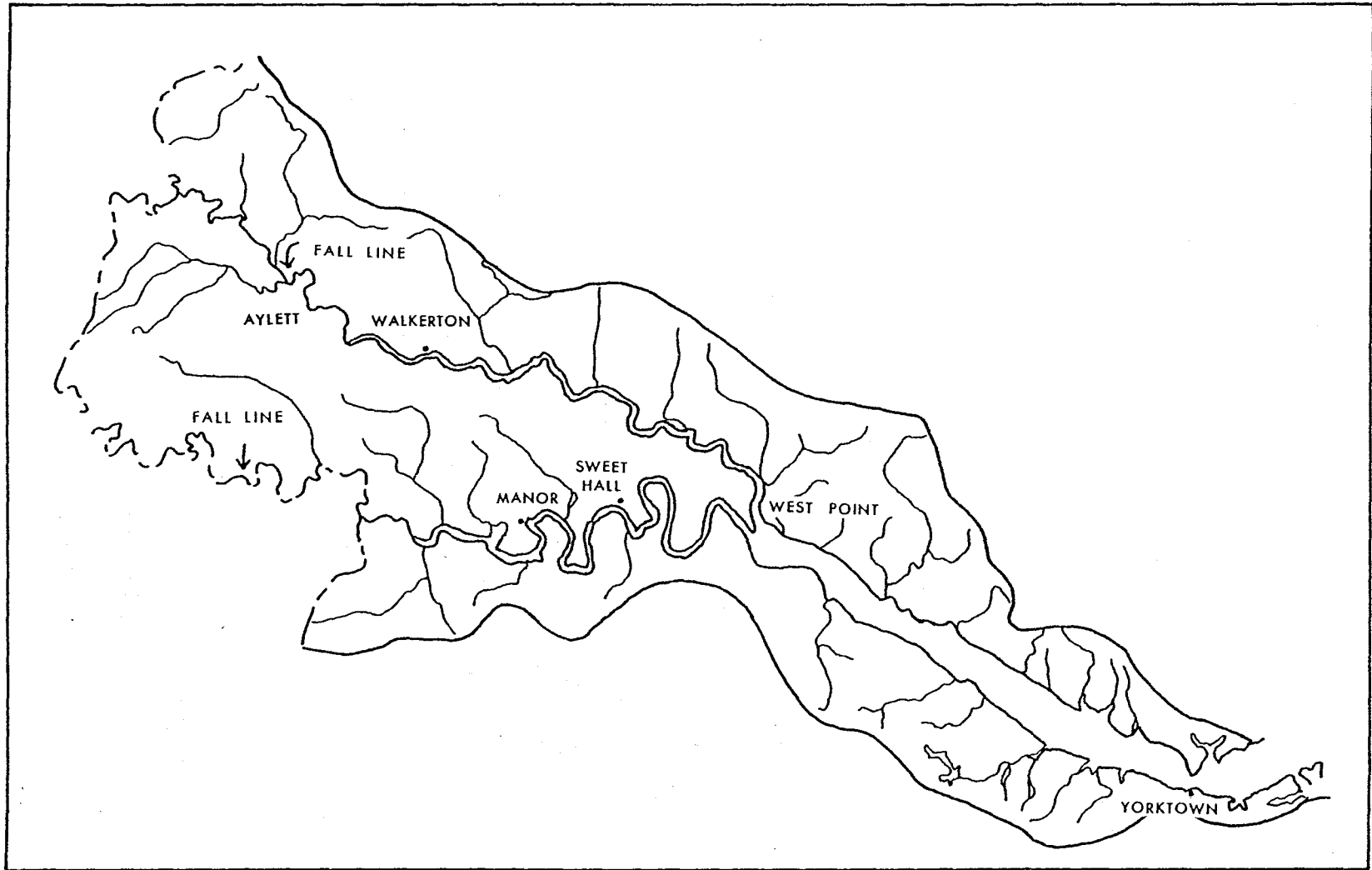


Figure 1. Downstream sub-basin of York drainage basin.

be greater than average in the period January - April and much less than average in July - September. The gauging station at Hanover has recorded historical extremes of 40,300 cfs ($1140 \text{ m}^3 \text{ sec}^{-1}$) and 12 cfs ($0.3 \text{ m}^3 \text{ sec}^{-1}$) with extremes at Beulahville of 16,900 cfs ($479 \text{ m}^3 \text{ sec}^{-1}$) and 5.9 cfs ($0.17 \text{ m}^3 \text{ sec}^{-1}$).

Tidal waves propagate upstream at approximately fourteen miles per hour although tidal patterns near the mouth are much more complicated (see Figure 2). As the tidal wave progresses, its amplitude increases. The mean tidal range is 2.2 feet (0.7 m) at Tue Marshes Light and 3.0 feet (0.9 m) at West Point. The tide range continues to increase in the tributaries, reaching 3.9 feet (1.2 m) at Walkerton in the Mattaponi and 3.3 feet (1.0 m) at Northbury in the Pamunkey. Tidal action ceases at the fall line, which is approximately three miles upstream of the Route 360 bridge in both the Mattaponi and Pamunkey Rivers. The tidal wave also undergoes a change in phase relationship. At Tue Marsh, low water occurs only about an hour after maximum ebb current, indicating an almost pure traveling wave. At West Point, this time difference is about two hours, indicating a shift toward standing wave characteristics. Average tidal current increases from 1.0 feet per second (30 cm/sec) near the mouth to 1.8 feet per second (54 cm/sec) near West Point but then decreases to 1.5 feet per second (46 cm/sec) at Walkerton and 0.8 feet per second (24 cm/sec) at Northbury.

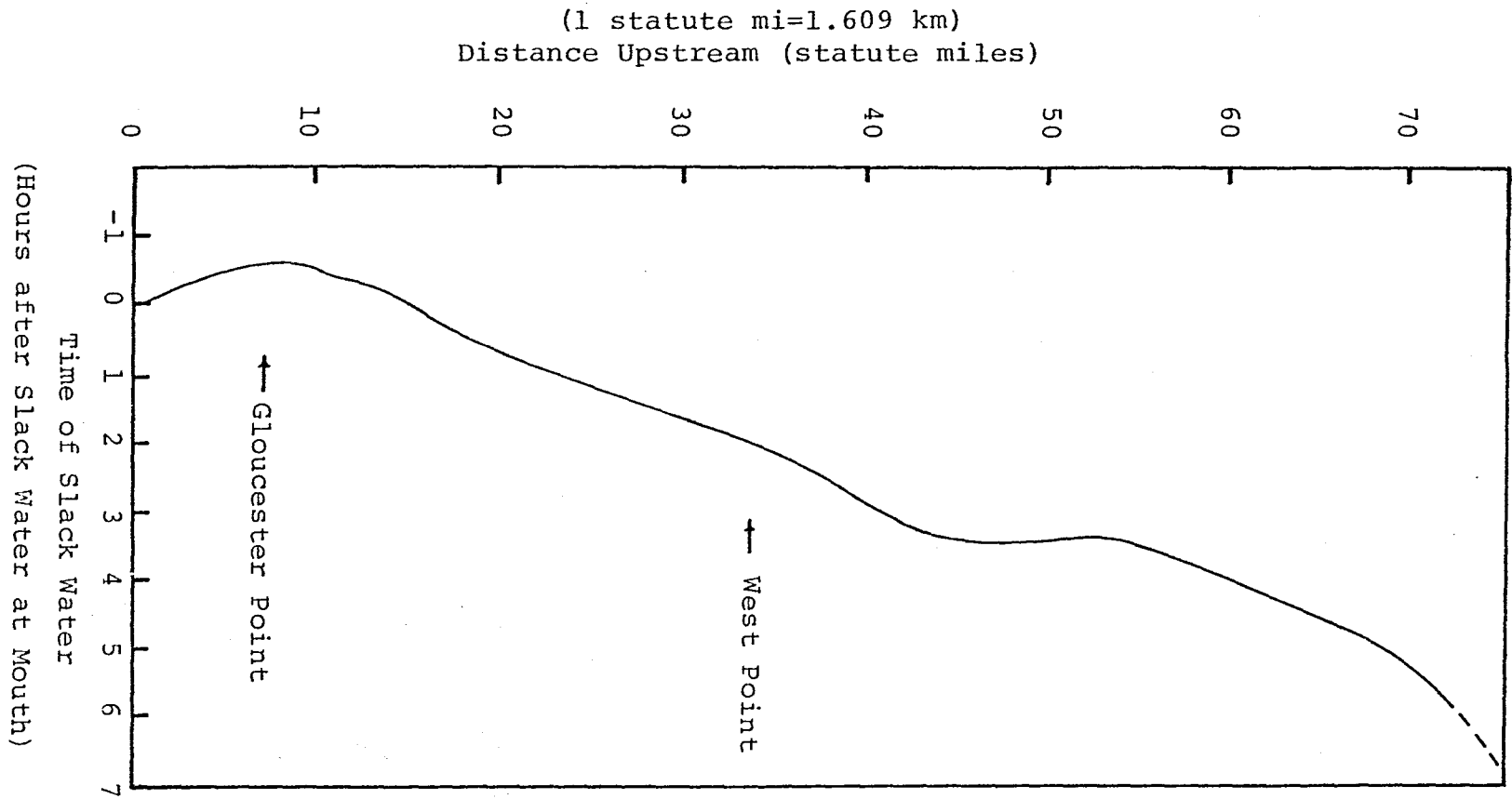


Figure 2. York and Pamunkey time of slack water relative to York River mouth.

Net tidal prism has been calculated from the intertidal volumes of Cronin (1971). Figure 3 shows net tidal prism versus distance upstream for the York. Although monotonic by definition, the tidal prism curves are not linear, but reflect the changes in tidal amplitude and stream geometry as the observer proceeds upstream.

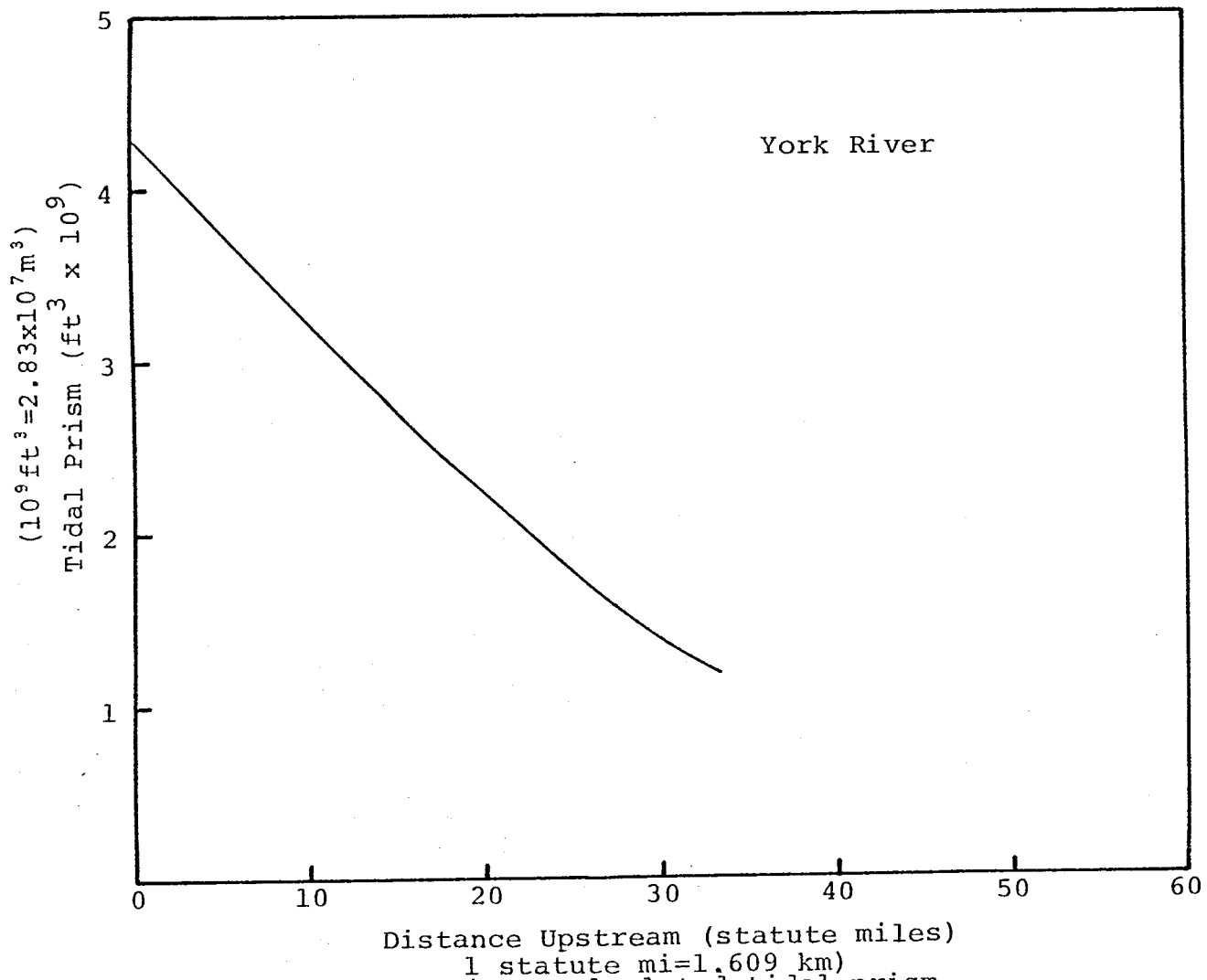


Figure 3. York River calculated tidal prism.

IV. DESCRIPTION OF THE WATER QUALITY MODEL

A. Biochemical Interactions

The model has ten components, i.e. ten dependent variables predicted as functions of space and time. Eight of these components interact (see Figure 4), with chlorophyll being the kingpin of the model. There are two closed nutrient cycles which begin and end at chlorophyll (here used as an index of phytoplankton biomass). In addition, the carbonaceous BOD-dissolved oxygen submodel interacts with chlorophyll through photosynthesis and respiration terms and with the nitrogen cycle through an oxidation term. Salinity is independent of the other components (apart from a weak influence on saturation concentration of dissolved oxygen) and bacteria is totally independent of the other components. For a discussion of parameters, see a description of the ecosystem model used for the Back and Poquoson Rivers (Hyer et al., 1977).

B. Hydraulic Processes

The model includes the following transport processes: longitudinal mean advection and gravitational circulation; longitudinal dispersion; lateral dispersion; vertical mixing and advection resulting from the gravitational circulation. The theories are given below.

1. Longitudinal

The freshwater discharge into the first reach is specified, as is the drainage area upstream of the first transect. This flow is partitioned among the

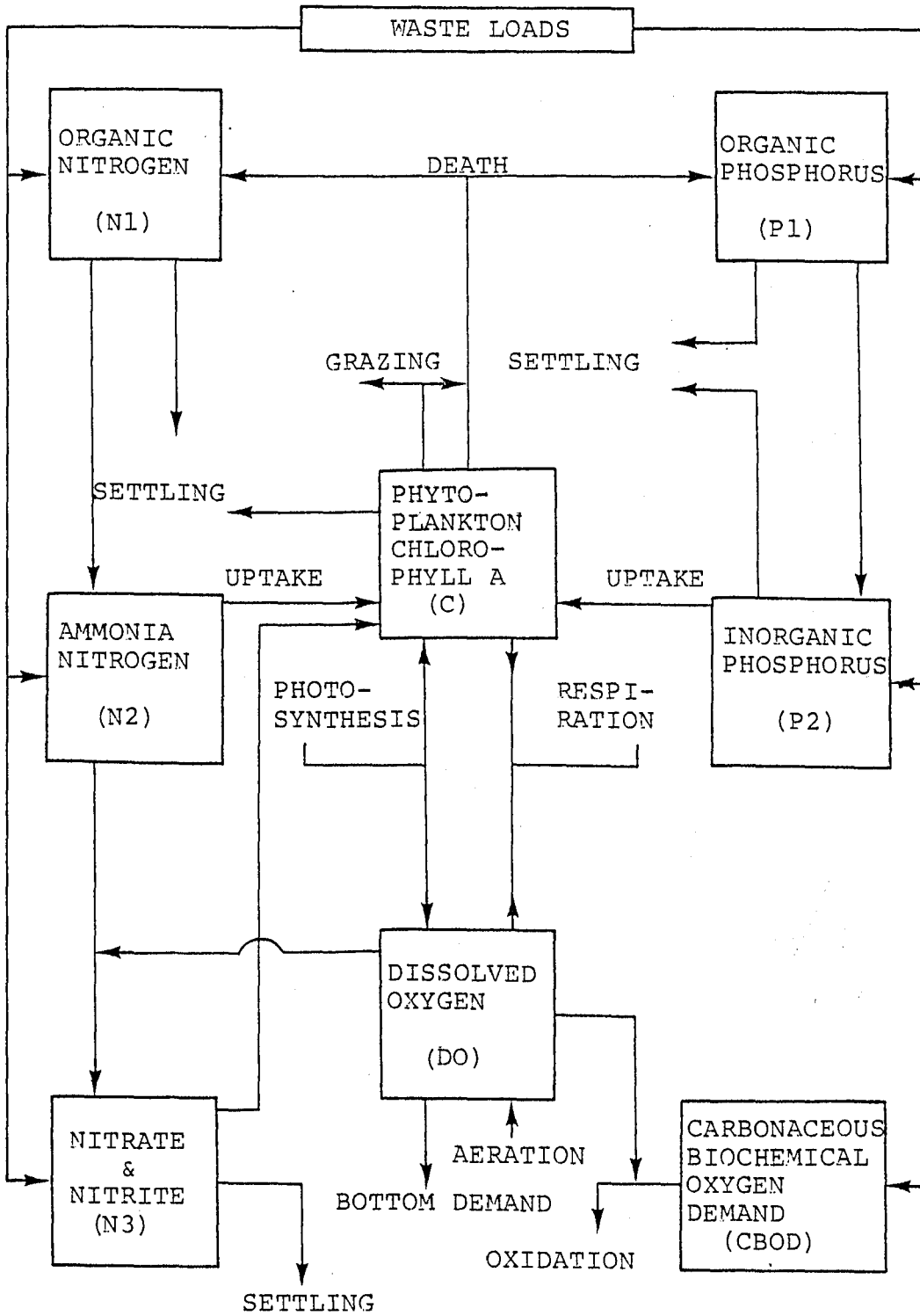


Figure 4. Flow diagram for ecosystem model.

six compartments according to partial cross-section areas in the farthest upstream transect. The drainage area of each reach is specified. Lateral inflow into each reach is calculated based on the assumption of equal runoff for equal area (hydrologic homogeneity). One-half of the lateral inflow is assigned to each side lateral division.

The gravitational circulation is driven by the haline structure and the equations used in the model are based on the theory of Hansen and Rattray (1965). They have derived the longitudinal transport in a stratified estuary as a function of depth. In the absence of wind stress, this transport is

$$\phi(\eta) = \frac{1}{2} (2 - 3\eta + \eta^3) + \frac{\nu Ra}{48} (\eta - 3\eta^3 + 2\eta^4)$$

where η is the dimensionless depth and νRa is a dimensionless parameter describing the intensity of estuarine gravitational circulation. Inspection of the velocity profile curves reveals that the dimensionless level of no motion is very nearly 0.5. However for real (non-rectangular) channels, the transport in the upper layer is:

$$Q_u = Q \left(\frac{11}{16} + \frac{\nu Ra}{192} f(\eta) \right)$$

where Q is the fresh water inflow and $f(\eta)$ is a function of the dimensionless depth, to be described under Method of Solution. The transport in the lower layer is then:

$$Q_L = Q - Q_u$$

The quantity νRa can be calculated from field data. Hansen and Rattray (1966) give the following relation:

$$\nu Ra = 16F_m^{-3/4}, \text{ where}$$

$$F_m = U_f / \sqrt{gh\Delta\rho/\rho}, \text{ a densimetric}$$

Froude number. The parameter F_m is calculated empirically for conditions at the mouth of the river. To allow for the streamwise variation of mean flow, the following equation is used:

$$Q_u = \begin{cases} Q \left(\frac{11}{16} + \frac{\nu Ra}{192} g\left(\frac{x}{L}\right) \right) & \text{for } x \leq L \\ \frac{11}{16} Q & \text{for } x > L \end{cases}$$

$g(\theta)$ is derived empirically and L is the intrusion length.

$$g(0) = 1, \text{ and}$$

$$g(1) = 0.$$

To extrapolate intrusion length from one condition to the general case, a scaling argument is used. According to Hansen and Rattray (1965):

$$L = \frac{QD}{BK_v} \frac{M}{v}$$

where M is a tidal mixing parameter, Q is fresh water flow, D is depth and B is width and K_v is the vertical turbulent mixing coefficient. From Hansen and Rattray (1966):

$$\frac{M}{v} \propto Q^{-7/5}, \text{ so that}$$

$$L \propto Q^{-2/5}.$$

The functional form of $g\left(\frac{x}{L}\right)$ was chosen in the process of model calibration to be:

$$g\left(\frac{x}{L}\right) = \sqrt{1 - \frac{x}{L}}; \quad x < L$$

Since gravitational circulation has been included explicitly, the corresponding dispersion coefficient (shear effect) should not be included, as it would have to be in a one-dimensional model. However, since tidal advection does not appear explicitly in the model, the so-called "phase effect" dispersion coefficient (Kuo & Fang, 1972) must be included. This mode of transport arises out of the combined effect of lateral variation in tidal current strength and lateral mixing. Salt, for example, is carried farther upstream in the center channel than along the shoals, during flood tide. Lateral mixing tends to spread this salt outward, toward the banks, where tidal current is weaker. On the subsequent ebb tide, this salt is not carried back as far as its origin. The net effect is a displacement upstream. This effect is approximated by a dispersion coefficient (Kuo & Fang, 1972).

$$E_t = \beta U_t \sqrt{\bar{A}}, \text{ where}$$

U_t is the magnitude of the tidal current, \bar{A} is the time-average cross-section area and β is an empirical constant of order unity.

2. Vertical

Vertical volume transport from the lower layer into the upper is calculated directly from the convergence of the mean flow in the lower layer. The vertical mixing coefficient is estimated by successive trial. Values tend to lie in the range 10^{-4} ft²/sec - 10^{-3} ft²/sec (0.09 - 0.9 cm²/sec).

3. Lateral

No lateral advection between compartments occurs in the model. However, lateral mixing is provided for. Holley, et al. (1970) have summarized the results of several previous investigations who have found the lateral dispersion coefficient C_y to be approximately

$$C_y = 0.067 RU, \text{ where}$$

R is the hydraulic radius and U is the shear velocity.

Using typical values for the York River estuary, the numerical result is of the order of 5 ft²/sec (4500 cm²/sec).

C. Method of Solution

The basic equation given in the previous sections must be put in a form suitable for digital computation. This means expressing the equations in finite-difference form,

so that they may be time-integrated using a digital computer. The water body must be conceptually broken down into control volumes, in each of which the water quality components are spatially averaged. Thus, the set of equations to be solved per time step is the number of control volumes (model compartments) multiplied by the number of components being modeled.

Each compartment exchanges material with the one above it or below it, with the one or two components beside it and with the compartments upstream and downstream from it. In generating the equations, each of these exchange rates must be expressed in terms of compartmental averages, a process necessarily involving approximations. Let a component C in the i th reach, j th position laterally and the ℓ th layer be represented by

$$C_{i,j,\ell}$$

The numbering scheme for compartments is shown in Figure 5.

$$1 \leq i \leq (i = 1 \text{ at upstream end})$$

$$j = 1 \text{ for south and west side}$$

$$j = 2 \text{ for center}$$

$$j = 3 \text{ for north and east side}$$

$$\ell = 1 \text{ for upper layer}$$

$$\ell = 2 \text{ for lower layer}$$

The lateral flux into the i, j, ℓ compartment from the $i, j-1, \ell$ compartment is

$$\frac{C_{i,j-1,\ell} - C_{i,j,\ell}}{W_{i,j-1,\ell}} L_i H_{i,j-1} E_{i,j-1}, \quad \text{where}$$

L_i is the length of the i th segment, $H_{i,j-1}$ is the depth of the interface between the $i, j-1, \ell$ compartment and the i, j, ℓ compartment and $W_{i,j-1,\ell}$ is the center-to-center distance. $E_{i,j-1}$ is the mixing coefficient between these two compartments. Naturally the mass balance for the $i, j-1, \ell$ compartment has a corresponding efflux.

There is both mixing and advection longitudinally. The transport into the i, j, ℓ compartment from the $i-1, j, \ell$ compartment is

$$\frac{C_{i-1,j,\ell} - C_{i,j,\ell}}{X_{i-1} - X_i} A_{i,j,\ell} E'_{i,j} \quad \text{where}$$

X_i is the distance, upstream from the mouth, of the center of the i^{th} segment, $A_{i,j,\ell}$ is the interface area between the $i-1, j, \ell$ compartment and the i, j, ℓ compartment and $E'_{i,j}$ is the mixing coefficient between the two compartments.

Advection transport includes the two-layer estuarine flow. Let the total mean freshwater flow into the $i, j, 1$ compartment and the $i, j, 2$ compartment be:

$$Q_{i,j}^m$$

Hansen and Rattray (1965) give the transport function for

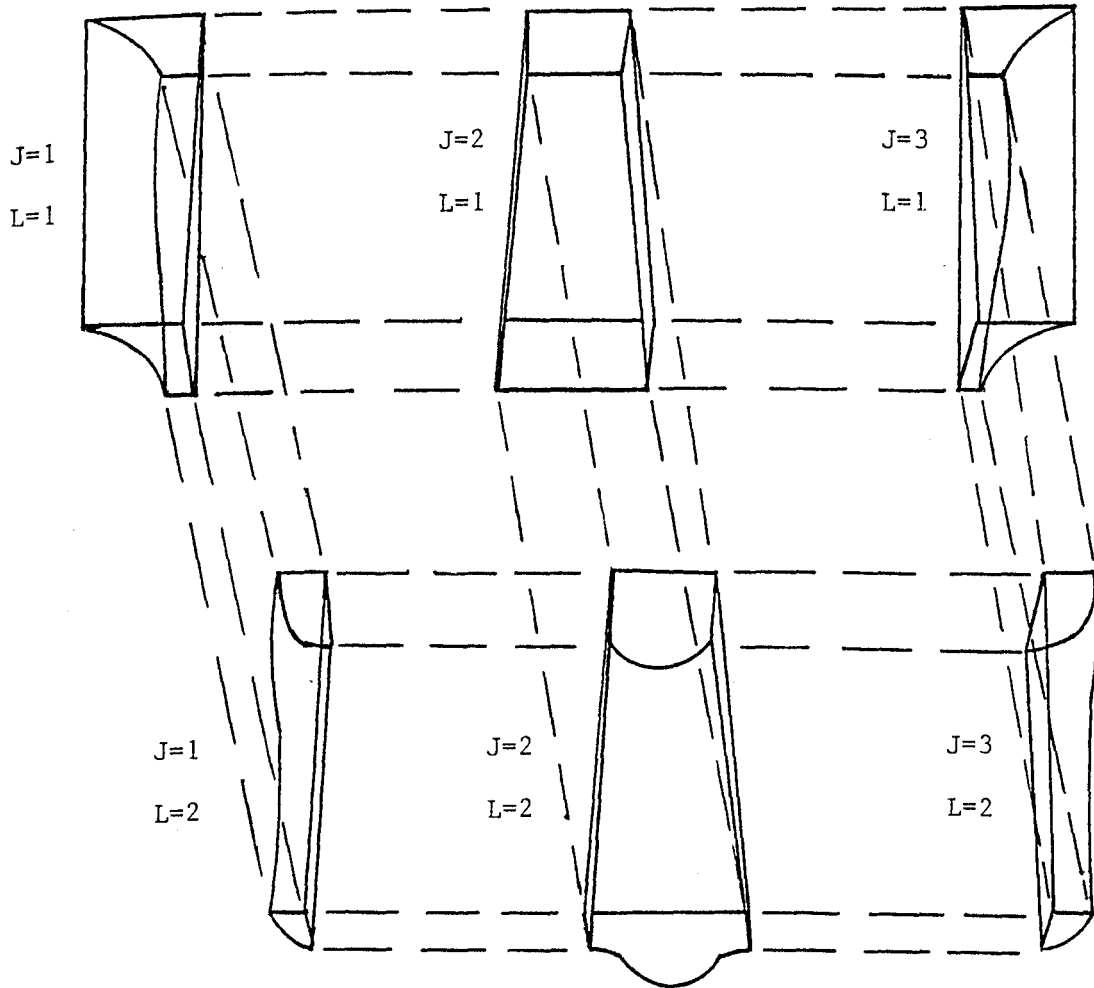


Figure 5. Exploded view of model segment showing numbering scheme for compartments.

gravitational circulation as

$$Q(\eta) = \frac{1}{2} (2 - 3\eta + \eta^3) - \frac{\nu Ra}{192} (4\eta - 12\eta^3 + 8\eta^4),$$

where νRa is a parameter expressing the strength of gravitational circulation and η is the dimensionless depth. This transport function can be written

$$Q(\eta) = P_1(\eta) - \frac{\nu Ra}{192} P_2(\eta)$$

The flow into the upper (i.e. $i, j, 1$) compartment is:

$$Q_{i,j,1} = Q_{m_{i,j}} \left(\frac{1 - P_1\left(\frac{Z_i}{H_j}\right) + \frac{\nu Ra}{192} P_2\left(\frac{Z_i}{H_j}\right) F\left(\frac{X_i}{L}\right)}{1 - P_1\left(\frac{H_j}{H}\right) + \frac{\nu Ra}{192} P_2\left(\frac{H_j}{H}\right) F\left(\frac{H_j}{L}\right)} \right)$$

where Z_i = depth from surface to interface between upper and lower layer;

H_j = total depth of upper and lower j th compartments combined;

H = $\max(H_1, H_2, H_3)$;

$$F\left(\frac{x}{L}\right) = \begin{cases} \sqrt{1 - \frac{x}{L}} & x \leq L \\ 0 & x > L \end{cases}$$

L = length scale for circulation.

Both Z_i and L are determined empirically. The flow into the lower compartment is:

$$Q_{i,j,2} = Q_{m_{i,j}} - Q_{i,j,1}$$

There is both advective transport and turbulent mixing between the upper and lower layers. The advective transport comes from the convergence of the flow in the lower layer, i.e.

$$q_{i,j} = Q_{i,j,2} - Q_{i+1,j,2}$$

The transport rate into the upper layer due to vertical mixing is:

$$\frac{C_{i,j,2} - C_{i,j,1}}{D_{i,j}} L_i W_i E''_{i,j} \quad \text{where}$$

$D_{i,j}$ is the vertical separation of the centers of the upper and lower compartments, W_i is the width of the interface and $E''_{i,j}$ is the mixing coefficient.

The integration scheme uses an implicit method for the biochemical terms and the longitudinal exchanges while calculating the lateral and vertical exchanges explicitly at the back time step. The finite difference equation for time step beginning at time t can be written:

$$\begin{aligned} \frac{C_{i,j,l}^{t+\Delta t} - C_{i,j,l}^t}{\Delta t} = & \frac{1}{2} (\alpha^t C_{i-1,j,l}^t + \beta^t C_{i+1,j,l}^t + \Gamma C_{i,j,l}^t \\ & + \alpha^{t+\Delta t} C_{i-1,j,l}^{t+\Delta t} + \beta^{t+\Delta t} C_{i+1,j,l}^{t+\Delta t} \\ & + \Gamma^{t+\Delta t} C_{i,j,l}^{t+\Delta t}) + \varepsilon^t (C_{i,j-1,l}^t - C_{i,j,l}^t) \\ & + \mu^t (C_{i,j+1,l}^t - C_{i,j,l}^t) \\ & + \nu^t (C_{i,j,3-l}^t - C_{i,j,l}^t) + J_{i,j,l}^t \end{aligned}$$

where α , β , Γ , ε , μ and ν are (possibly time-dependent) known expressions and J is the source term, including both external loadings and transmutations from other components. The factor

Γ includes the first-order decay rate, if any. If all the terms containing $t+\Delta t$ (i.e. the quantities yet unknown at time t) are isolated on one side of the equation, the result is:

$$\begin{aligned}
 & C_{i,j,\ell}^{t+\Delta t} \left(1 - \frac{\Gamma^{t+\Delta t} \Delta t}{2}\right) - C_{i-1,j,\ell} \frac{\alpha^{t+\Delta t} \Delta t}{2} \\
 & - C_{i+1,j,\ell} \frac{\beta^{t+\Delta t} \Delta t}{2} \\
 = & C_{i,j,\ell}^t \left(1 + \frac{\Gamma^t \Delta t}{2}\right) + C_{i-1,j,\ell}^t \frac{\alpha^t \Delta t}{2} \\
 & + C_{i+1,j,\ell}^t \frac{\beta^t \Delta t}{2} + (C_{i,j+1,\ell}^t - C_{i,j,\ell}^t) \mu^t \Delta t \\
 & + (C_{i,j-1,\ell}^t - C_{i,j,\ell}^t) \varepsilon^t \Delta t \\
 & + (C_{i,j,3-\ell}^t - C_{i,j,\ell}^t) \nu^t \Delta t + J_{i,j,\ell}^t
 \end{aligned}$$

The unknown on the left-hand side of the equation are interconnected and must be solved simultaneously. This kind of system of equations is called "tridiagonal" due to the pattern made when the equations are expressed in matrix form. The special fast method for solving this kind of system is found elsewhere (Fang, et al., 1973).

D. Evaluation of Parameters and Rate Constants

1. Hydraulic Inputs

a. Freshwater Inflow. The York is formed by the confluence of the Mattaponi and Pamunkey Rivers. Both of these streams are gauged; the Mattaponi at Beulahville and the Pamunkey at Hanover. The records for these gauging stations for the months of June through September, 1976, are shown in Table 1. For model operation these flows were averaged for the month period prior to the day on which the survey was conducted and were augmented to include the lateral inflow occurring between the gauging station and the transect farthest upstream. Finally, the Mattaponi flow went into the J=3 compartment while the Pamunkey flow was divided equally between the J=1 and J=2 compartments.

b. Longitudinal Dispersion Coefficient. The formula used is given in a previous section. The constant β was found to give the best results when set at 2. The dispersion coefficient then turns out to be in the range 500-1000 ft²/sec.

c. Circulation Parameter. The input constant $\nu R a$ indicates the strength of the density-induced circulation. This parameter and the input β were simultaneously adjusted to reproduce the observed salinity. The final value of $\nu R a$ was 100.

2. Biochemical Inputs

a. Reaeration Coefficient k_2 . O'Connor and Dobbins (1956) presented a theoretical derivation of the reaeration coefficient, in which fundamental turbulence parameters were

TABLE 1. Flow Records for Beulahville
and Hanover, Virginia, 1976

Date	Beulahville (Mattaponi)				Hanover (Pamunkey)			
	June	July	Aug.	Sept.	June	July	Aug.	Sept.
1	367	260	110	58	860	257	151	174
2	369	190	90	53	1020	246	154	137
3	401	160	72	62	1080	237	153	187
4	467	140	60	67	1010	224	148	183
5	442	120	56	66	641	219	137	162
6	358	120	50	57	475	202	134	150
7	297	130	46	49	366	210	129	147
8	258	160	47	45	349	226	125	151
9	237	190	123	41	325	221	246	151
10	200	190	249	43	305	244	269	150
11	179	170	207	65	289	256	226	136
12	163	180	131	61	259	265	183	120
13	155	160	91	52	248	259	159	109
14	145	150	74	46	263	237	168	110
15	142	140	123	48	285	224	180	119
16	137	120	188	385	277	261	598	521
17	154	150	176	836	329	305	501	627
18	203	240	171	1010	468	257	281	413
19	216	420	133	878	612	223	208	321
20	245	250	100	585	581	223	175	267
21	311	160	81	371	597	210	160	193
22	292	130	69	247	893	198	146	159
23	277	110	61	187	1790	182	143	141
24	287	95	55	148	1240	177	129	140
25	293	90	50	123	830	168	124	143
26	367	80	47	109	820	165	112	148
27	473	78	43	107	1470	177	112	179
28	510	76	49	314	665	169	124	830
29	429	78	64	340	299	160	154	579
30	342	110	69	273	259	162	165	329
31	---	140	65	---	---	159	171	---
Min.	137	76	43	41	248	159	112	109
Mean	291	154	95.2	224	630	217	189	241
Max.	510	420	249	1010	1790	305	598	830

taken into account. They derived the following formula:

$$(k_2)_{20} = \frac{(D_c U)^{1/2}}{H^{3/2}}$$

where D_c is the molecular diffusivity of oxygen in water, U and H are the cross-sectional mean velocity and depth respectively, and $(k_2)_{20}$ is the reaeration coefficient at 20°C . This formula has been shown to give a satisfactory estimate of k_2 for a reach of river with cross-sectional mean depth and velocity more or less uniform throughout the reach. However, this formula must be modified when dealing with two layered systems. The factor $H^{3/2}$ appearing in the denominator must be broken into two factors.

$$H^{3/2} = H_s^{1/2} H_v, \text{ where}$$

H_v is the mean depth of the volume to which oxygen is being replenished. In the two layered model $H_v = H_1$, i.e., the mean depth of the upper layer. The other depth, H_s is the characteristic depth of the vertical shear of the horizontal flow. This depth will have an intermediate value between the depth of the upper layer and the total depth. Hence,

$$H_s = H_1 + 0.5 H_2,$$

i.e., the depth of the upper layer plus half the depth of the lower layer, will be approximately correct.

To adjust k_2 for temperatures other than 20°C , Elmore and West's (1961) formula is used

$$k_2 = (k_2)_{20} \cdot 1.024^{(T-20)}$$

where T is the water temperature in centigrade degrees.

b. CBOD Oxidation Rate, k_1 . The oxidation rate of CBOD (carbonaceous biochemical oxygen demand) normally ranges from 0.1 to 0.5 per day. The rate also depends on water temperature; the following formula is used for this temperature dependence,

$$k_1 = (k_1)_{20} \cdot 1.047^{(T-20)}$$

c. Saturated Oxygen Content, DO_s . The saturation concentration of dissolved oxygen depends on temperature and salinity. From tables of saturation concentration (Carritt and Green, 1967) a polynomial equation was determined by a least-squares method.

$$\begin{aligned} \text{DO}_s = & 14.6244 - 0.367134T + 0.0044972T^2 \\ & - 0.0966S + 0.00205TS + 0.0002739S^2 \end{aligned}$$

where S is salinity in parts per thousand and DO_s is in mg/liter.

d. Benthic Oxygen Demand, BEN. The bottom sediment of an estuary may vary from deep deposits of sewage or industrial waste origin to relatively shallow deposits of natural material of plant origin and finally to clean rock and sand. The oxygen consumption rate of the bottom deposits

must be determined with field measurements. Field data were obtained in the summer of 1976 (see Table 2). Sampling locations are shown in Figure 6. A value of $1.0 \text{ gm/m}^2/\text{day}$ at 20°C is typical average for most estuaries. The temperature effect was simulated by thomann, 1972.

$$\text{BEN} = (\text{BEN})_{20} \cdot 1.065^{(T-20)}$$

where $(\text{BEN})_{20}$ is the benthic demand at 20°C .

e. Coliform Bacteria Dieoff Rate, k_b .

$$k_b = (k_b)_{20} \cdot 1.040^{(T-20)}$$

where $(k_b)_{20}$ is the dieoff rate at 20°C and T is temperature in degrees centigrade. The normal range of $(k_b)_{20}$ is 0.5-4.0/day.

f. Settling Rate of Organic Nitrogen, k_{n11} .

k_{n11} is of order of 0.1/day

g. Organic N to NH_3 Hydrolysis Rate, k_{n12} .

$$k_{n12} = aT$$

where a is of order of 0.007/day/degree.

h. NH_3 to NO_3 Nitrification Rate, k_{n23}

$$k_{n23} = aT$$

where a is of order of 0.01/day/degree.

TABLE 2. Benthic Oxygen Demand Studies
York River, 1976

Date	Station	Benthic Oxygen Demand (gm/m ² /day)
25 June	7A	1.6
25 June	7B	3.4
2 July	5A	1.5
2 July	1B	0.9

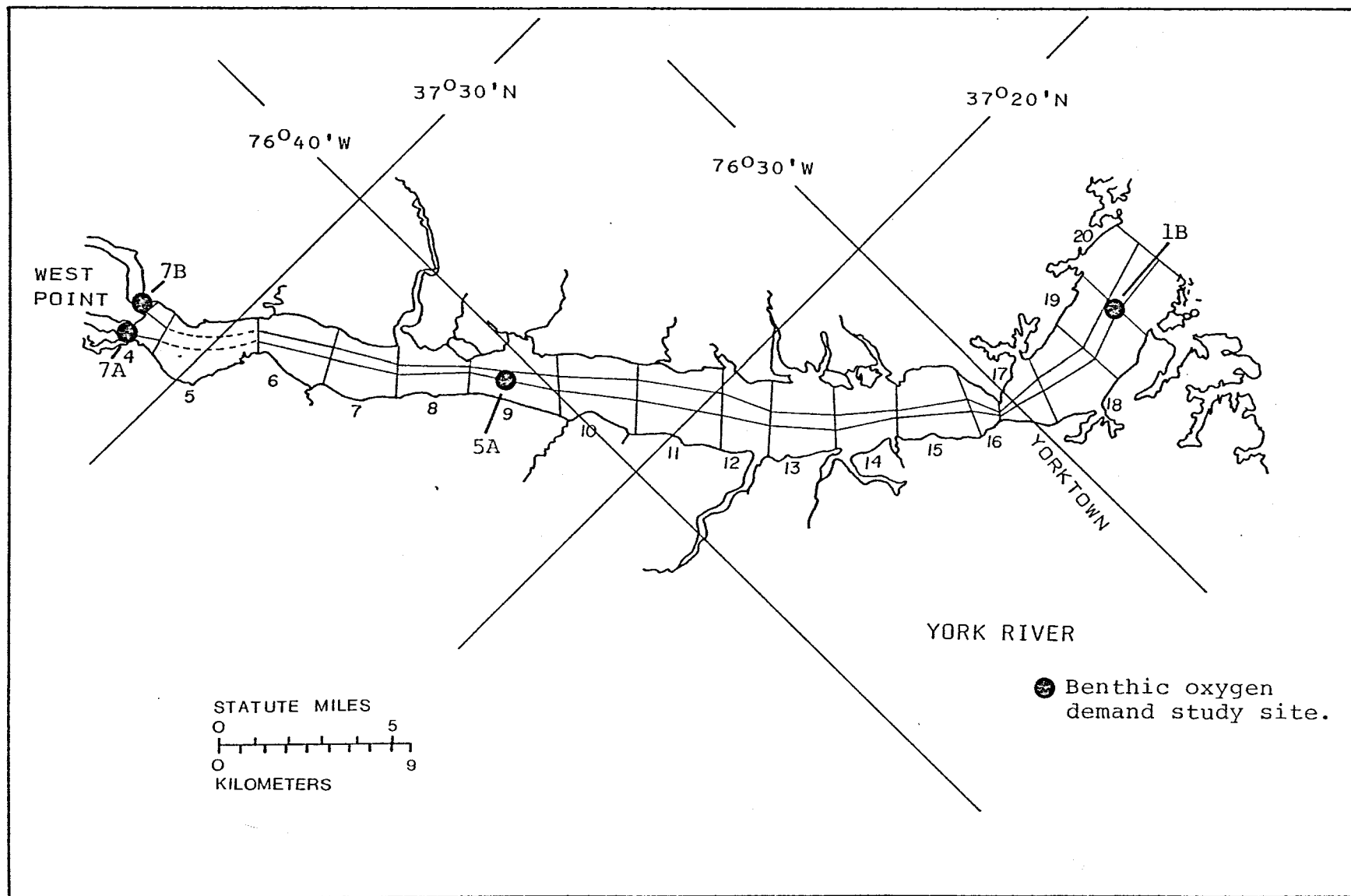


Figure 6. The York River showing model segments and benthic oxygen demand sampling sites.

i. NO_3 Escaping Rate, k_{n33}

k_{n33} is usually negligible.

j. Organic Phosphorus Settling Rate, k_{p11}

k_{p11} is order of 0.1/day.

k. Organic P to Inorganic P Conversion Rate, k_{p12}

$$k_{p12} = aT$$

where a is of order of 0.007/day/degree.

l. Inorganic Phosphorus Settling Rate, k_{p22}

k_{p22} is of order of 0.1/day.

m. Nitrogen-chlorophyll Ratio, a_n

a_n is of order of 0.01 mg N/ μg C.

n. Phosphorus-chlorophyll Ratio, a_p

a_p is of order of 0.001 mg P/ μg C.

o. Carbon-chlorophyll Ratio, a_c

a_c is of order of 0.05 mg carbon/ μg C.

p. Oxygen Produced Per Unit of Chlorophyll Growth, a_d

$$a_d = 2.67 \cdot a_c \cdot PQ$$

where PQ is photosynthesis quotient, $PQ = 1 \sim 1.4$.

q. Oxygen Consumed Per Unit of Chlorophyll Respired,
 a_r

$$a_r = 2.67 \cdot a_c / RQ$$

where RQ is respiration ratio.

r. Phytoplankton Settling Rate, k_{cs}

$$k_{cs} = S_\ell / h$$

where S_ℓ is settling velocity, whose normal range is 15 to 150 cm/day (0.5 to 5 ft/day) and h is the hydraulic depth.

s. Zooplankton Grazing, Kg. In reality, Kg should depend on the concentration of herbivorous zooplankton biomass. This effect has been included in the grazing rate.

t. Endogenous Respiration Rate, R_s

$$R_s = aT$$

where a is of order of 0.005/day/degree.

u. Growth Rate, G_c . The growth rate expression is that developed by Di Toro, O'Connor and Thomann (1971) and as used in this model is given by

$$G_c = k_{gr} T \cdot I (I_a, I_s, k_e, C, h) \cdot N (N_2, N_3, P_2)$$

temperature effect	light effect	nutrient effect
-----------------------	-----------------	--------------------

where k_{gr} is the optimum growth rate of the order of 0.1/day/degree. The functional form, I, for the light effect incorporates

vertical extinction of solar radiation and self-shading effect.

The form is

$$I = \frac{2.718}{k_e h} (e^{-\alpha l} - e^{-\alpha_0})$$

$$k_e = k_e' + 0.0088 \cdot C + 0.054 \cdot C^{0.66}$$

$$\alpha l = \frac{I_a}{I_s} e^{-k_e h}$$

$$\alpha_0 = \frac{I_a}{I_s}$$

k_e' is the light extinction coefficient at zero chlorophyll concentration, k_e is the overall light extinction coefficient, I_a is the incoming solar radiation and I_s is the optimum light intensity, about 300 langleys per day. The nutrient effect makes use of product Michaelis - Menton kinetics and is given by

$$N = \frac{N_2 + N_3}{K_{mn} + N_2 + N_3} \cdot \frac{P_2}{K_{mp} + P_2}$$

where K_{mn} is the half saturation concentration for total inorganic nitrogen and K_{mp} is the half saturation concentration for phosphorus. K_{mn} and K_{mp} have been reported to be about 0.3 - 0.4 and 0.03 - 0.05 mg/l respectively, although K_{mn} has been reported as low as 0.008 mg/l and K_{mp} has been reported as low as 0.015 mg/l.

V. MODEL CALIBRATION AND VERIFICATION

A. Calibration Procedure

Before a model can be applied to future predictions, it must be tested and proved capable of reproducing actually observed conditions. Many input constants will be modified in this successive approximation process. These constants are ones that have not been measured directly, but only approximated from existing literature. When one set of field data has been predicted by the model, the model is said to be calibrated. The next step is to keep the same set of input constants and attempt to reproduce a second set of field data. Once this has been done successfully, the model is said to be verified. When verification is first attempted, there is normally a need to readjust some inputs in order to improve the verification without compromising the calibration.

The York ecosystem model was calibrated according to field data collected June 15-16 and July 1-2, 1976. Since manpower and boats were limited and the area to be studied large, the river was covered in two parts. The original schedule for field sampling called for the second portion of the survey to be conducted immediately after the first half. However, 1.4" of rainfall were recorded at West Point on June 17, 1976. There was additional rain for several days, followed by a several day dry period and then 1.5" of rain on June 26. No additional rainfall was recorded between June 26 and the second portion of the field survey. Model segmentation is

shown in Figure 6. The calibration results for the center channel are shown in Figures 7 to 16. The error bars in these figures represent standard error of the mean. Part of the point source data was supplied by Betz Engineers through the Hampton Roads Water Quality Agency. The rest came from data compiled by the Water Control Board and used in the calibration of an earlier model (Hyer, et al., 1975). Point source data are shown in Table 3.

Verification data consisted of a slack water run made on September 13, 1976. Samples were taken at low water slack as it progressed upstream. The samples were taken between 10:00 a.m. and 2:00 p.m. and so the model prediction was made at high noon, model time. Results are shown in Figures 17 to 25. Fecal coliform is not included since the data are inadequate for comparison.

B. Model Sensitivity

One way of judging whether a model is reliable is to see if it can reproduce a known set of conditions (verification). Another check of a model is to see if variations in input cause any difference in output. This quality of a model is called sensitivity. A model which gives essentially the same result no matter what the input is clearly of little use in projections, unless there is good reason to believe that the real estuary ("prototype") is just as insensitive as the model indicates. The model inputs of most concern are:

- point source loadings (since this is chiefly what projections are about);

York River Salinity Calibration

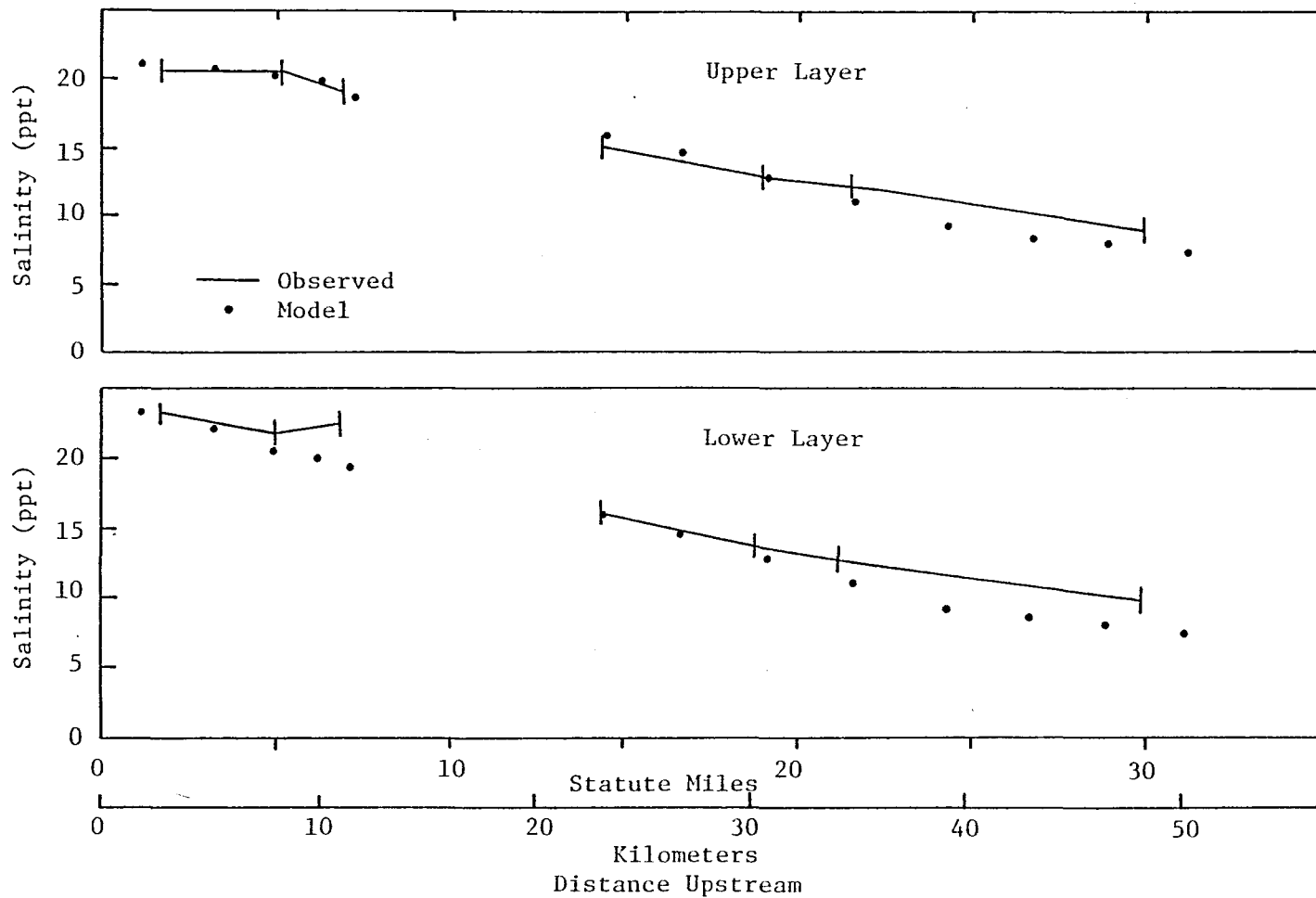


Figure 7. York River salinity calibration results.

York River Organic Nitrogen Calibration

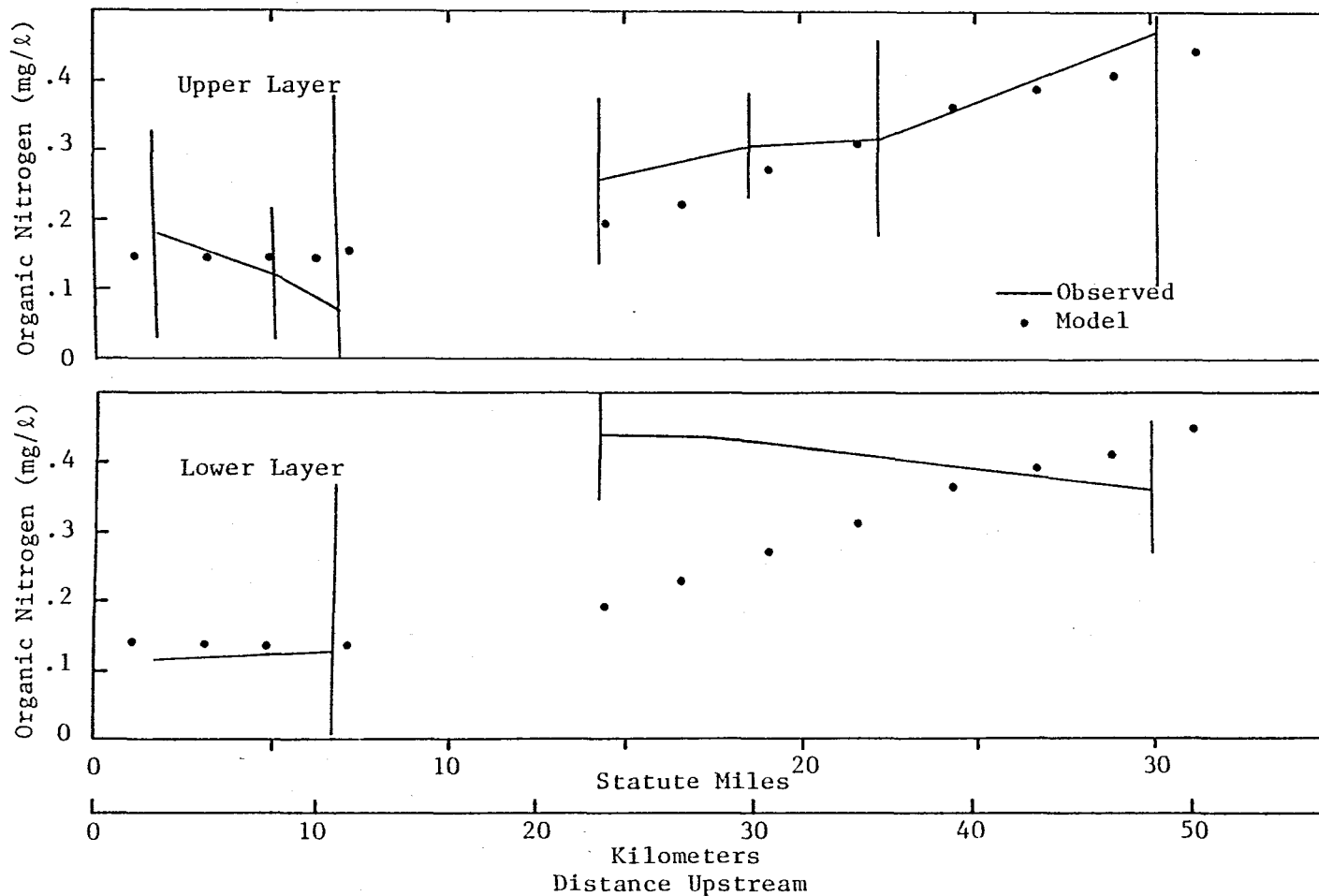


Figure 8. York River organic nitrogen calibration results.

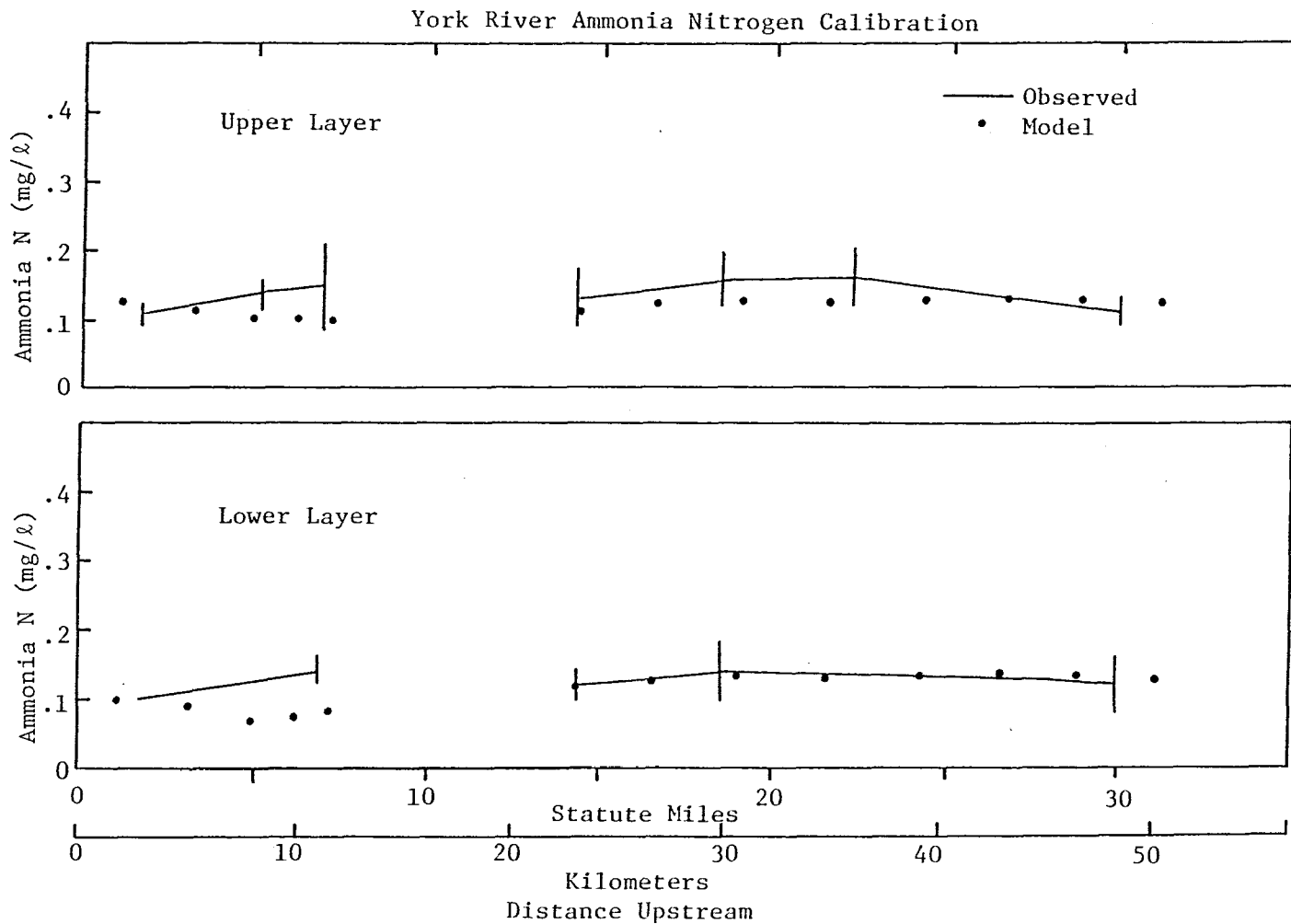


Figure 9. York River ammonia nitrogen calibration results.

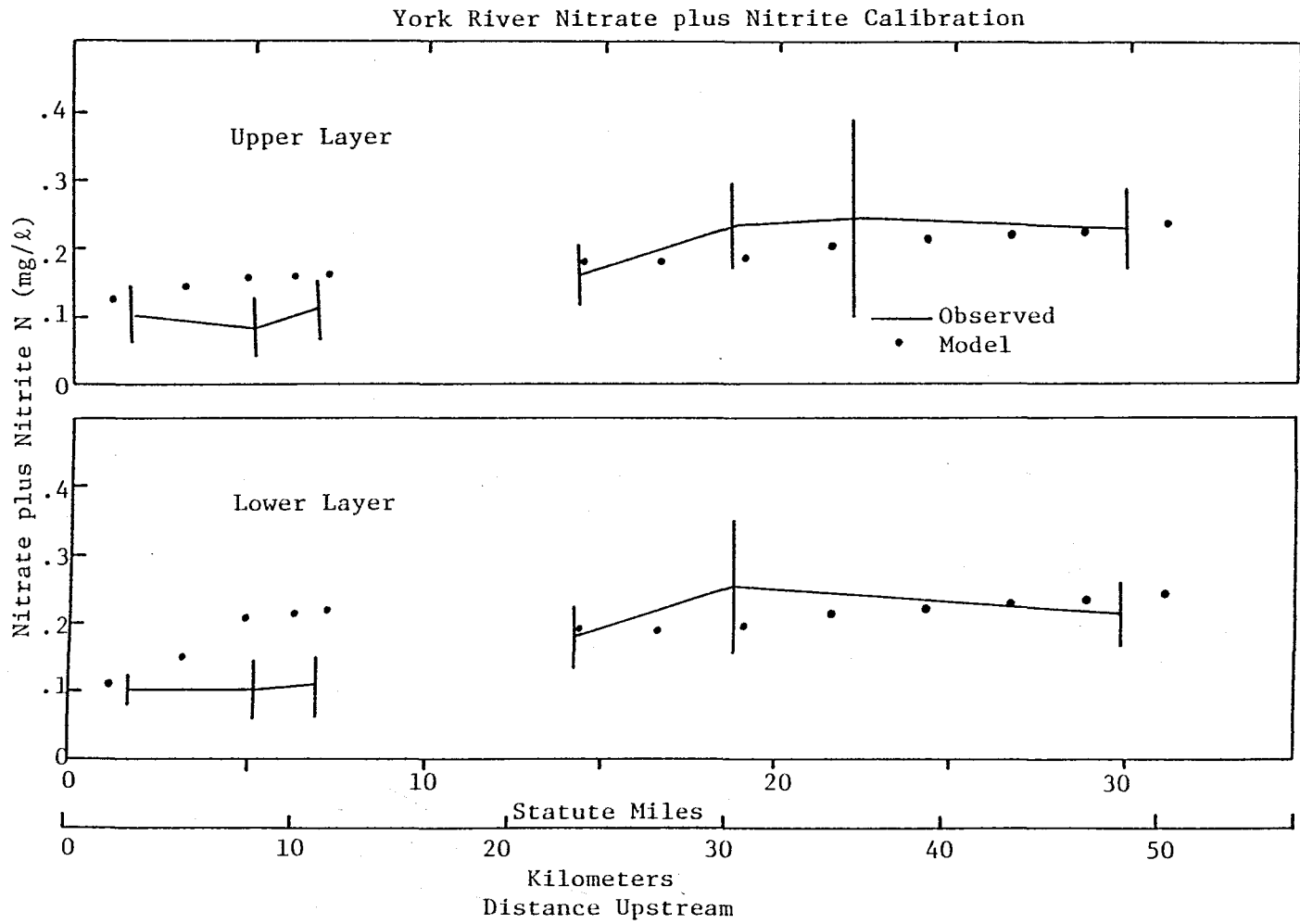


Figure 10. York River nitrate plus nitrite calibration results.

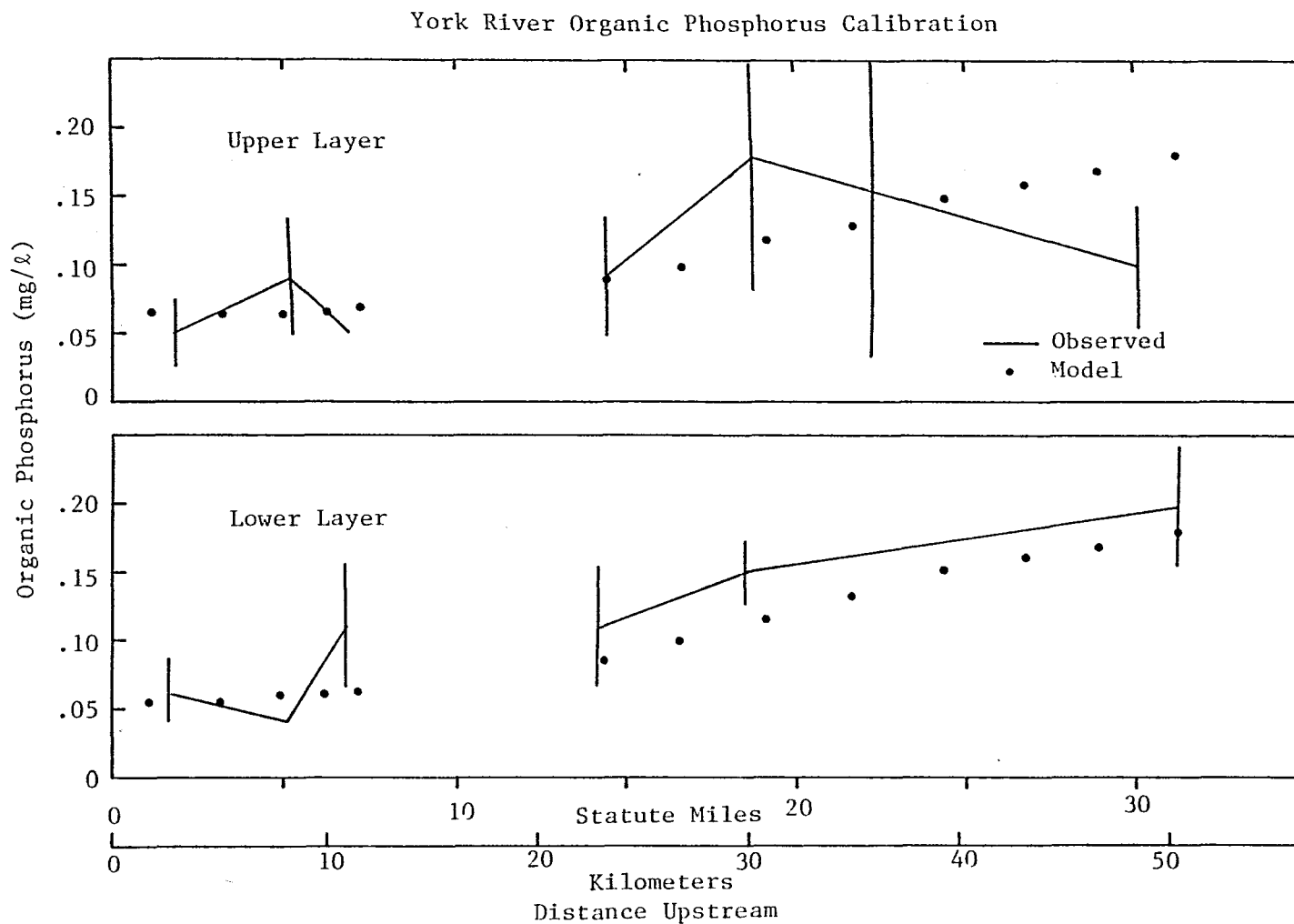


Figure 11. York River organic phosphorus calibration results.

York River Inorganic Phosphorus Calibration

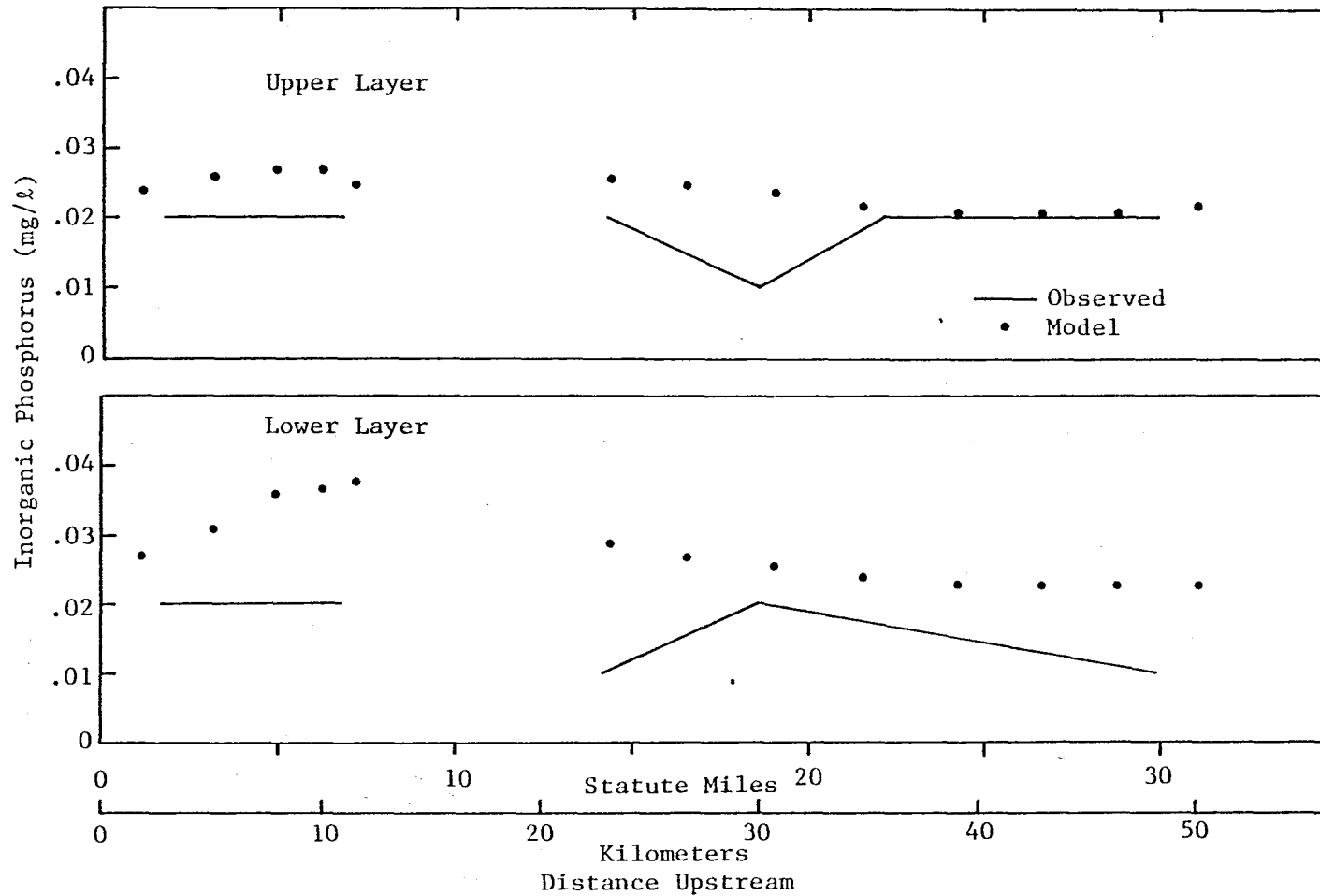


Figure 12. York River inorganic phosphorus calibration results.

York River Chlorophyll Calibration

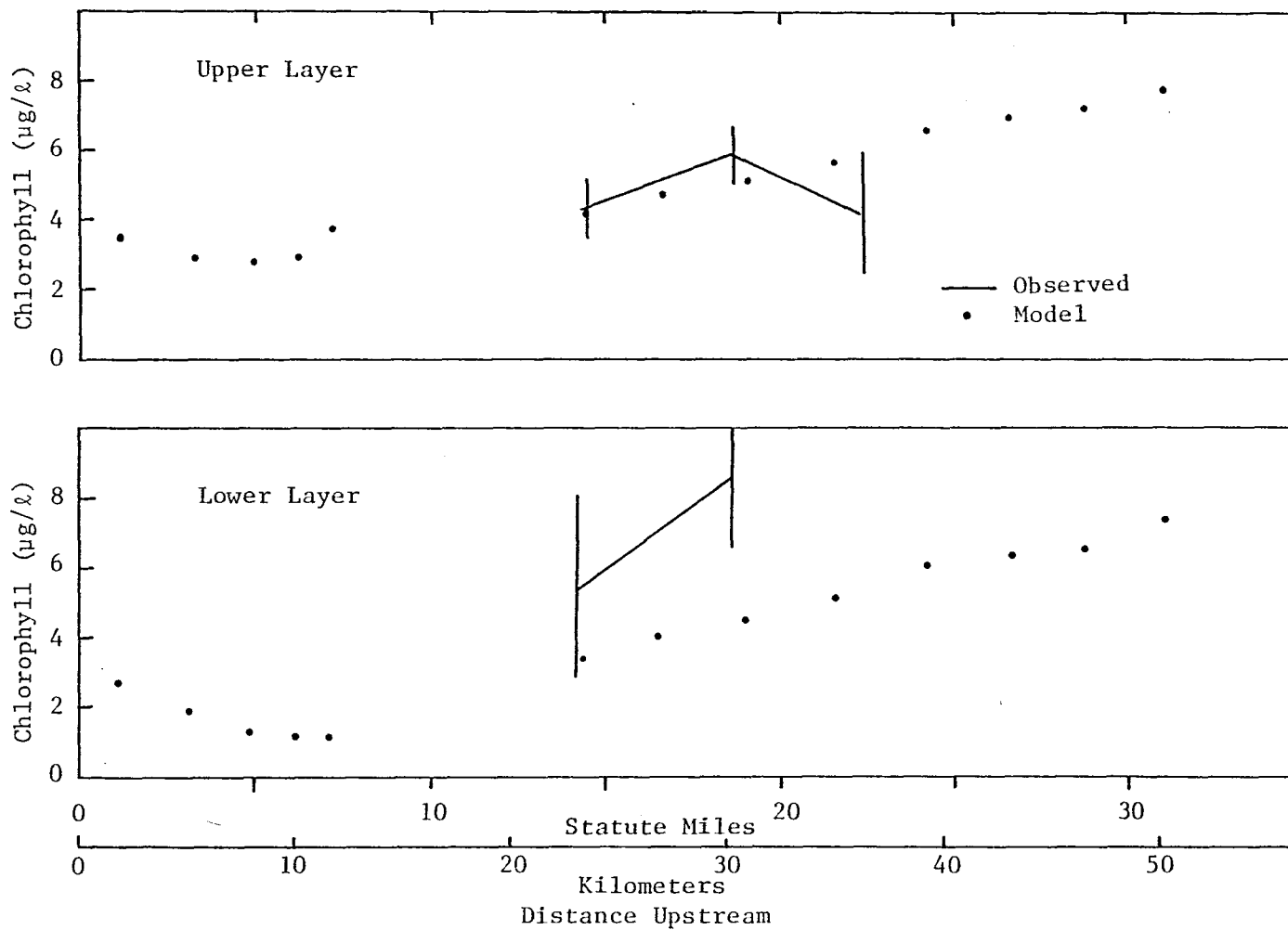


Figure 13. York River chlorophyll 'a' calibration results.

York River CBOD Calibration

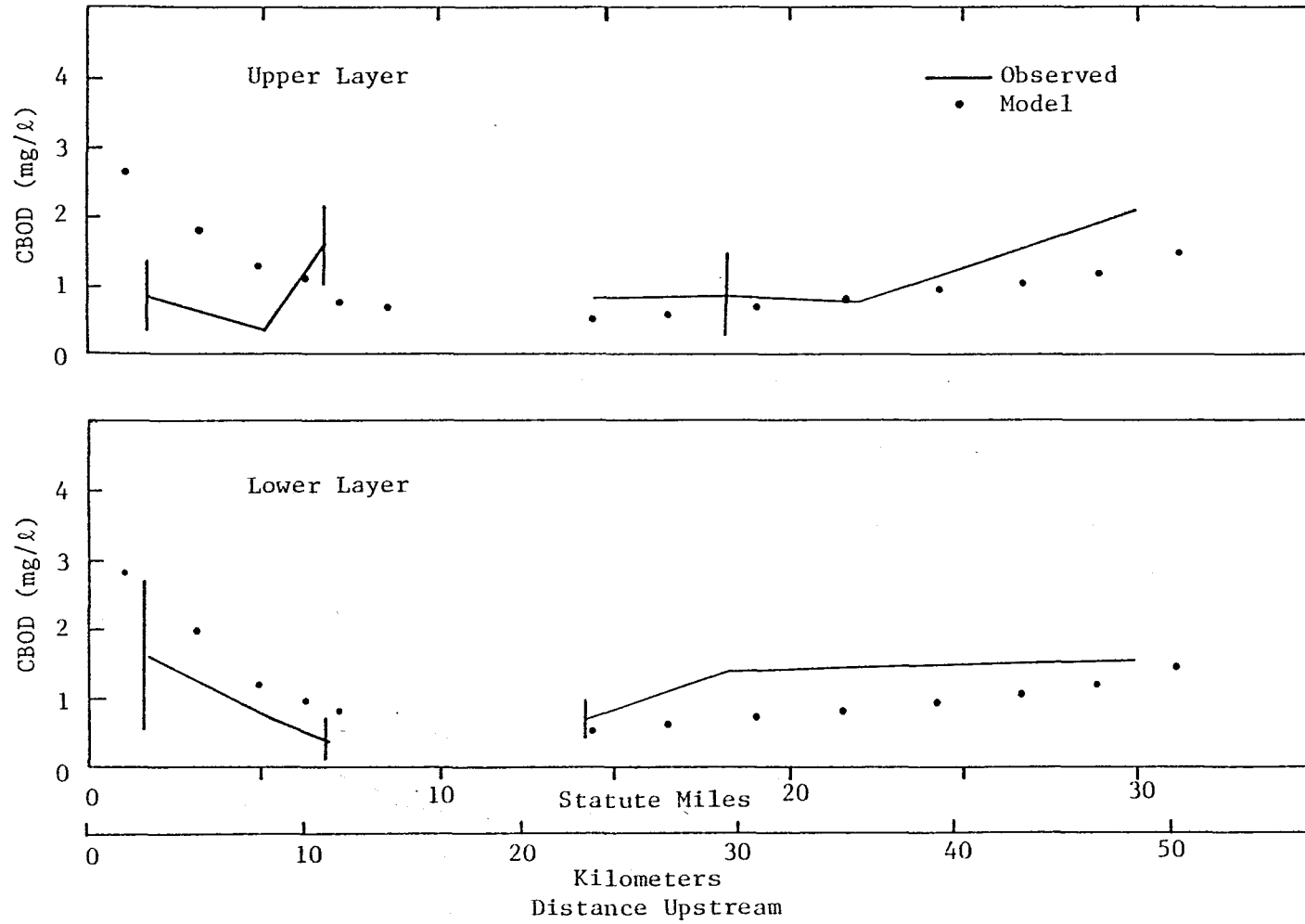


Figure 14. York River carbonaceous BOD calibration results.

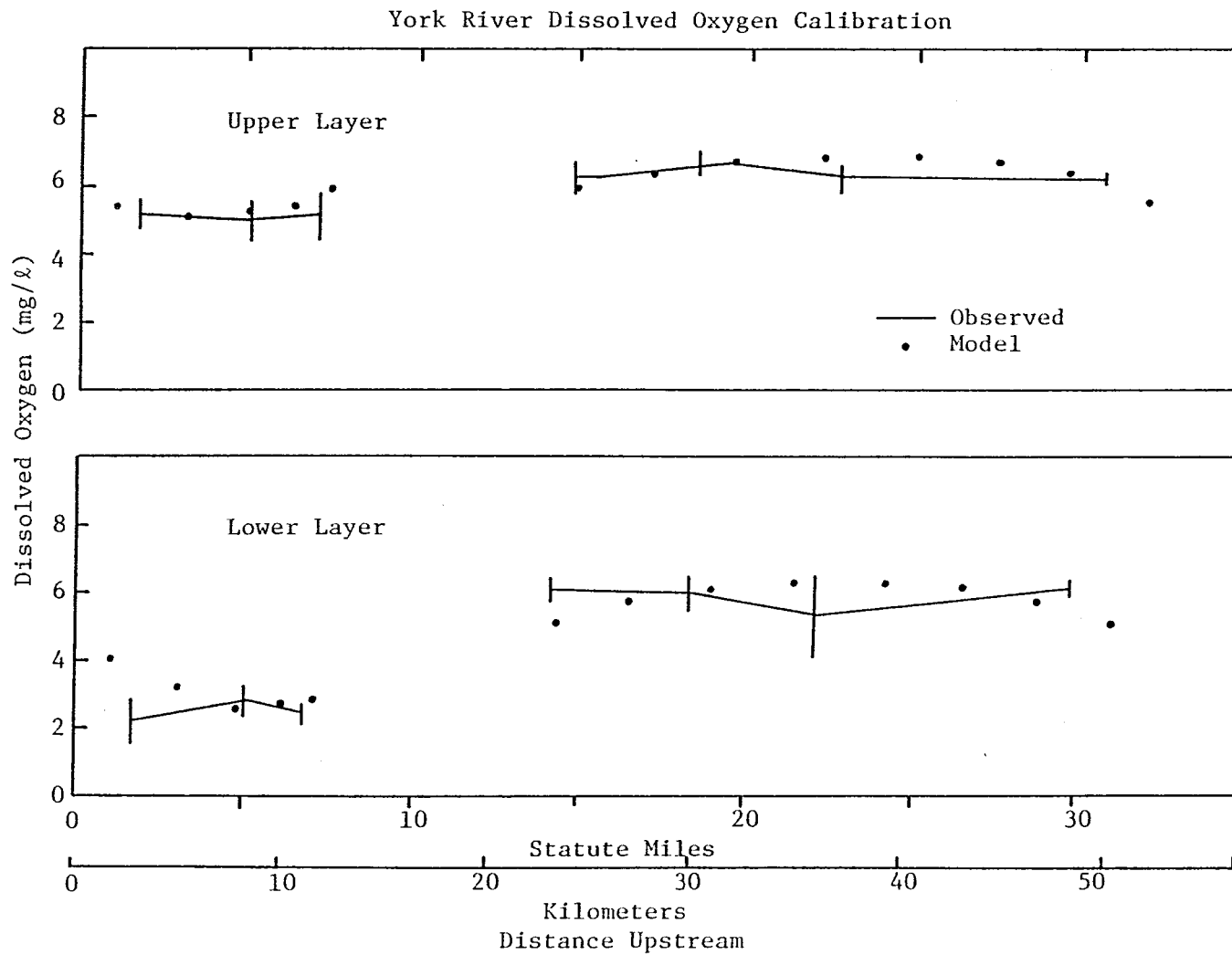


Figure 15. York River dissolved oxygen calibration results.

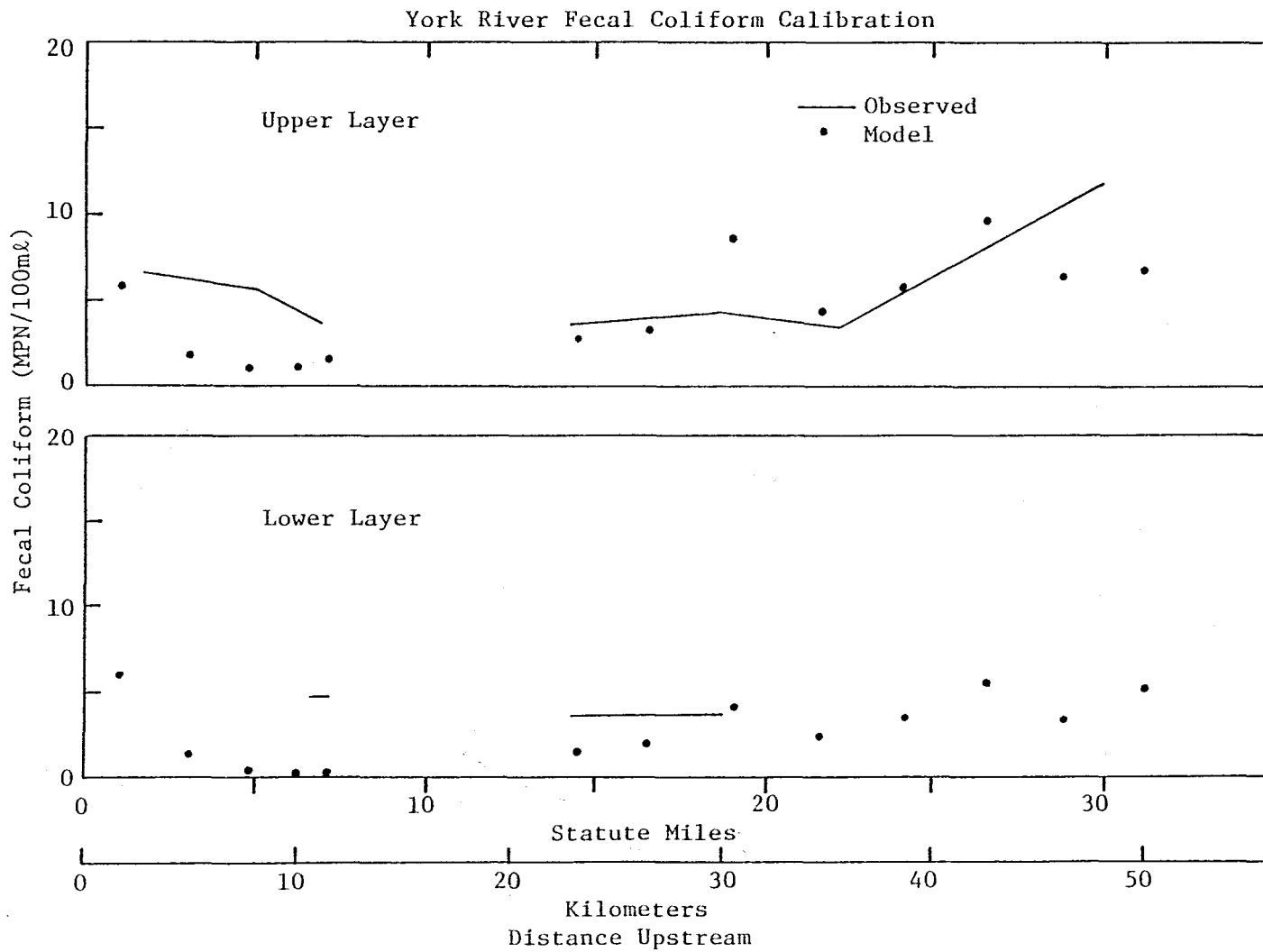


Figure 16. York River fecal coliform calibration results.

TABLE 3. Point Sources of Loading Used in Calibration and Verification

Name	Lateral Segment Number	Longitudinal Segment Number	Flow (cfs)	BOD ₅ (lb/day)	Organic N (lb/day)	Ammonia (lb/day)	NO ₂ and NO ₃ (lb/day)	Organic P (lb/day)	Inorganic P (lb/day)	Coliform (billions per day)
AMOCO ¹	1	20	2.7	1169.	182.	525	12.9	12.9	38.7	3.8
VEPCO ¹	1	19	3.7	37.	42.	42.	3.0	1.2	0.3	2.9
Yorktown Nat'l Park ²	1	17	0.1	108.	3	3	3	3	3	3
Naval Weapons ₂ Station	1	14	0.6	132.	3	3	3	3	3	3
Camp Peary ²	1	13	0.1	18.	3	3	3	3	3	3
Town of Toano ²	1	5	<0.1	17.	3	3	3	3	3	3

¹ Data supplied by Betz Environmental Engineers.

² Data from Hyer, et al., 1975.

³ Nutrient and bacterial data not available.

York River Salinity Verification-LWS September 13, 1976

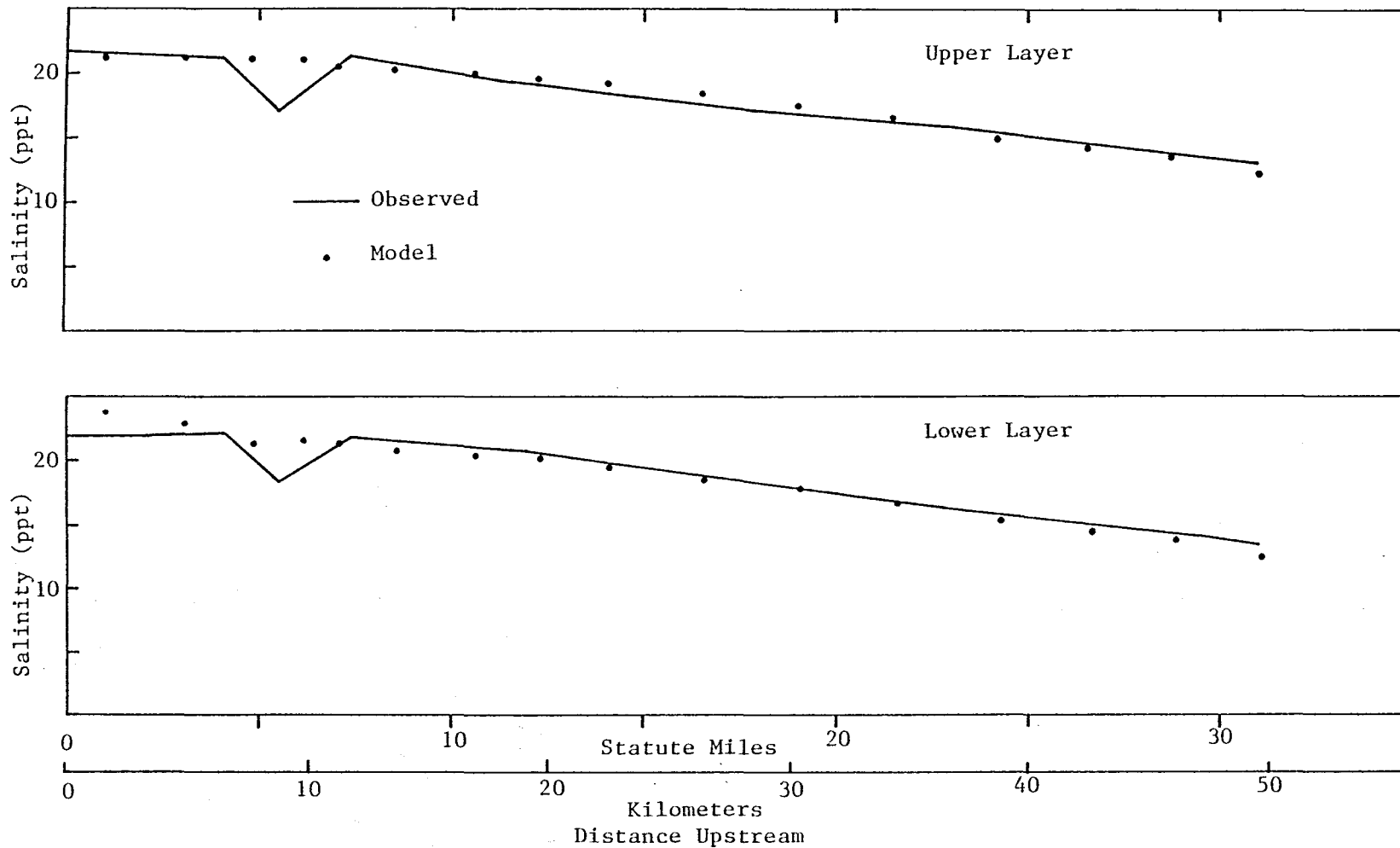


Figure 17. York River salinity verification.

York River Organic Nitrogen - LWS Sept. 13, 1976

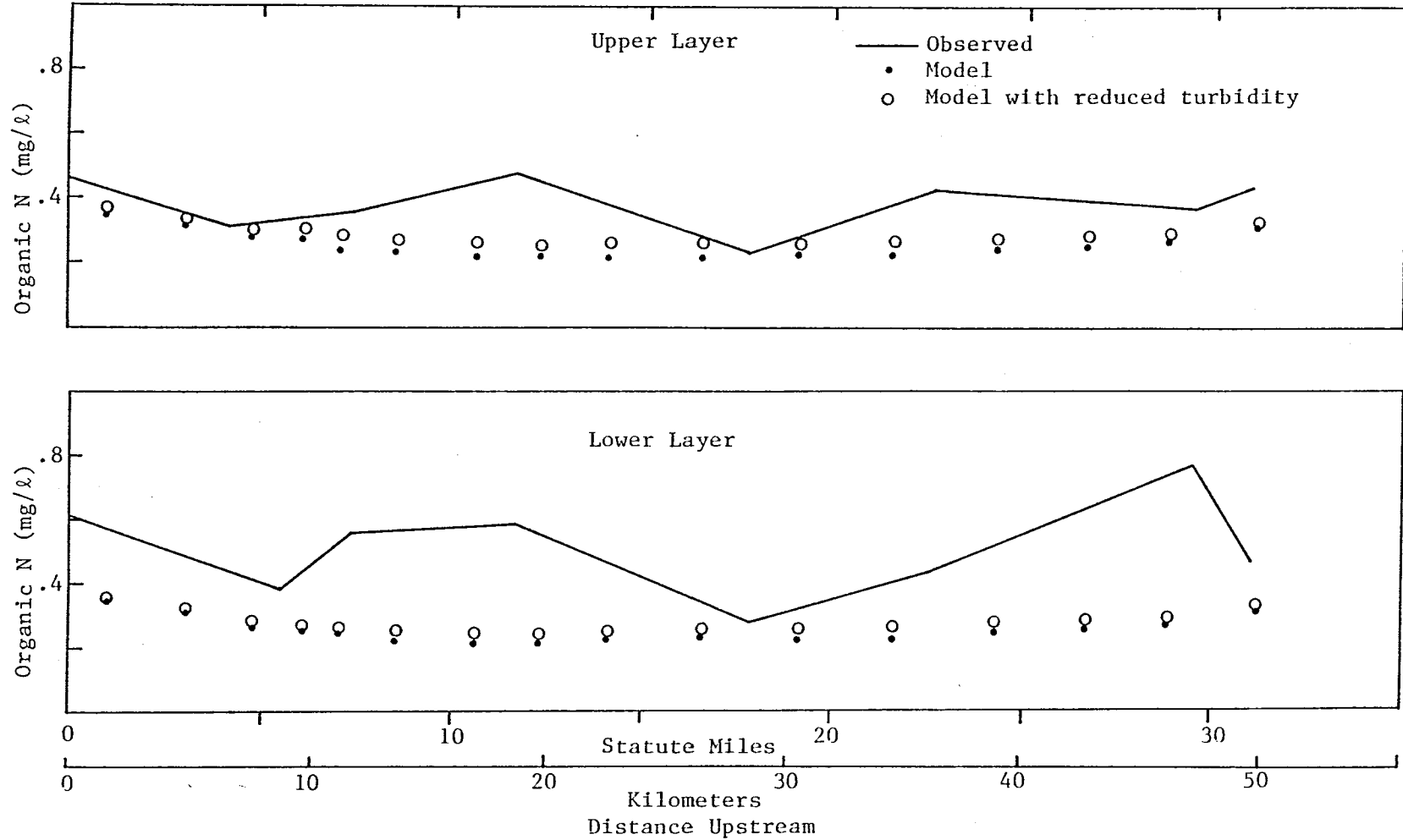


Figure 18. York River organic nitrogen verification.

York River Ammonia Nitrogen - LWS Sept. 13, 1976

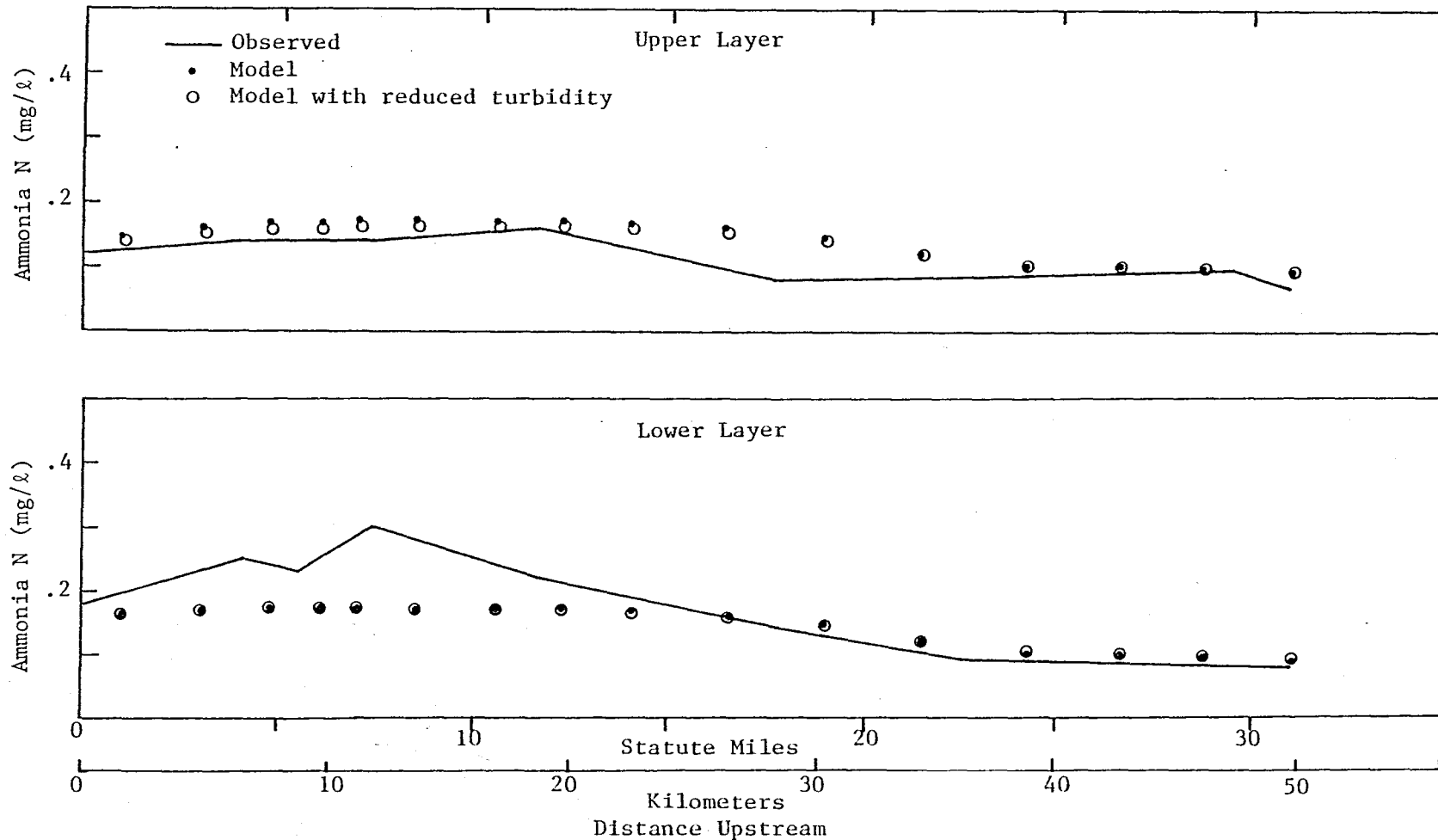


Figure 19. York River ammonia nitrogen verification.

York River Nitrate plus Nitrite - LWS Sept. 13, 1976

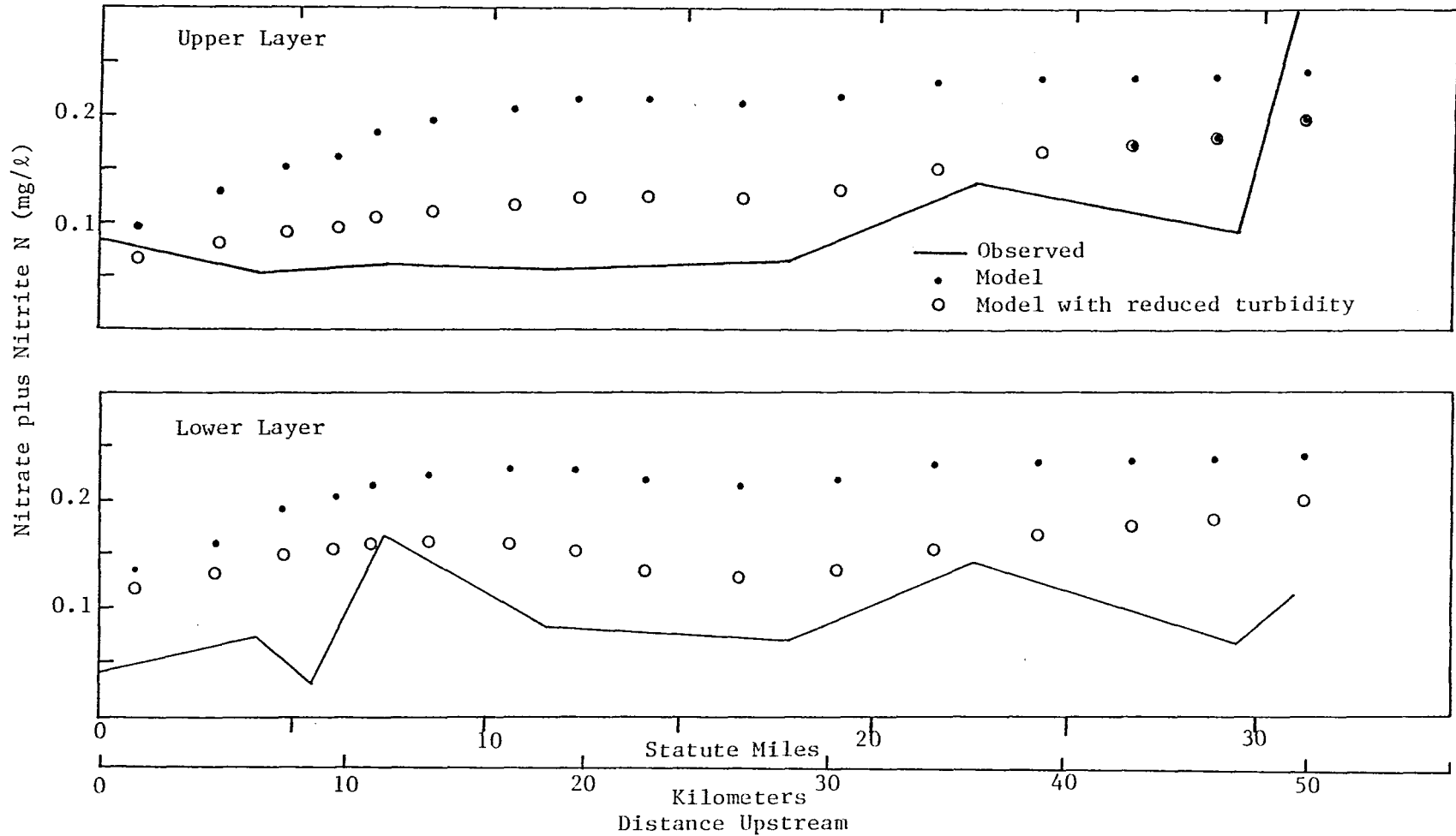


Figure 20. York River nitrate plus nitrite verification.

York River Organic Phosphorus - LWS Sept. 13, 1976

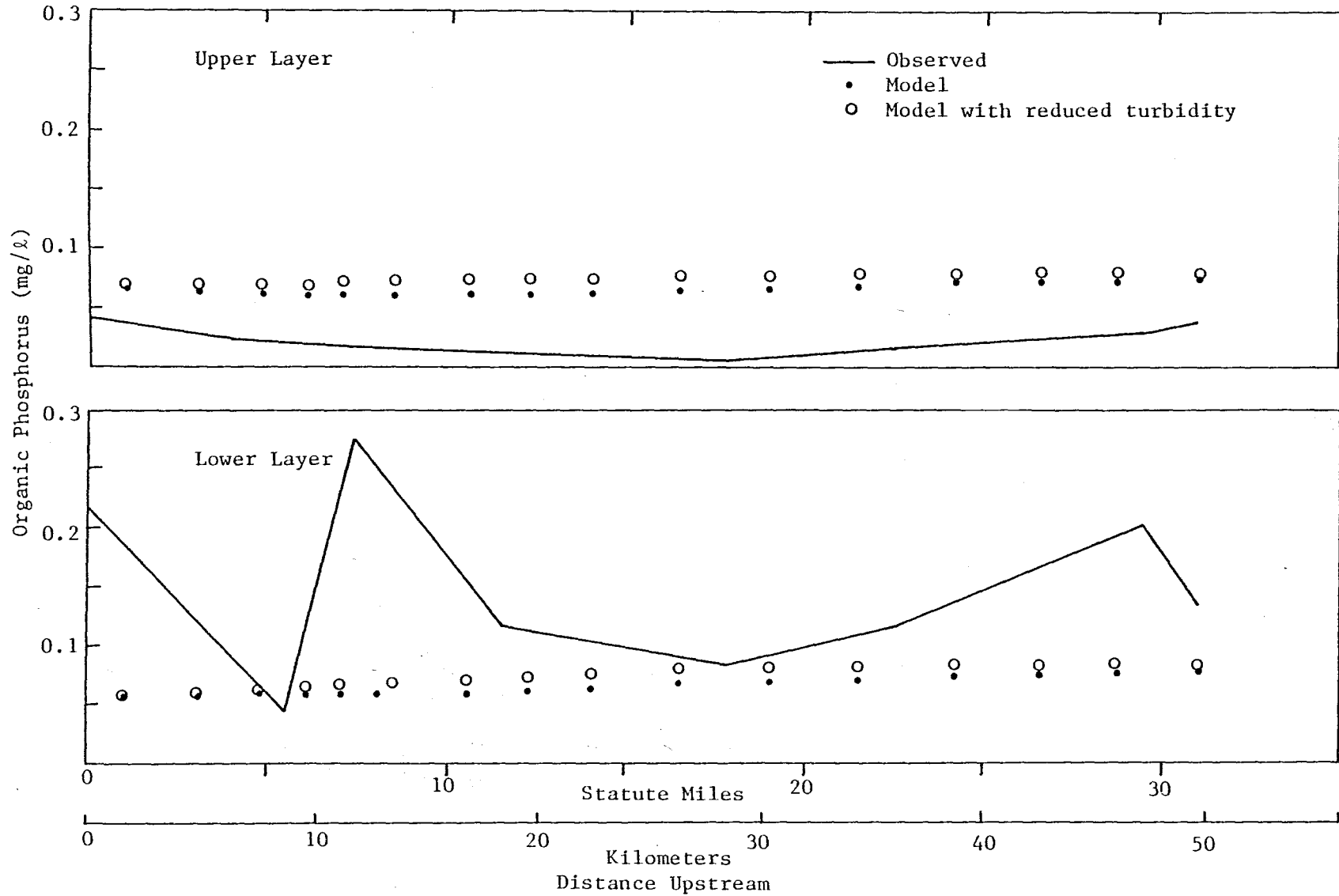


Figure 21. York River organic phosphorus verification.

York River Inorganic Phosphorus - LWS Sept. 13, 1976

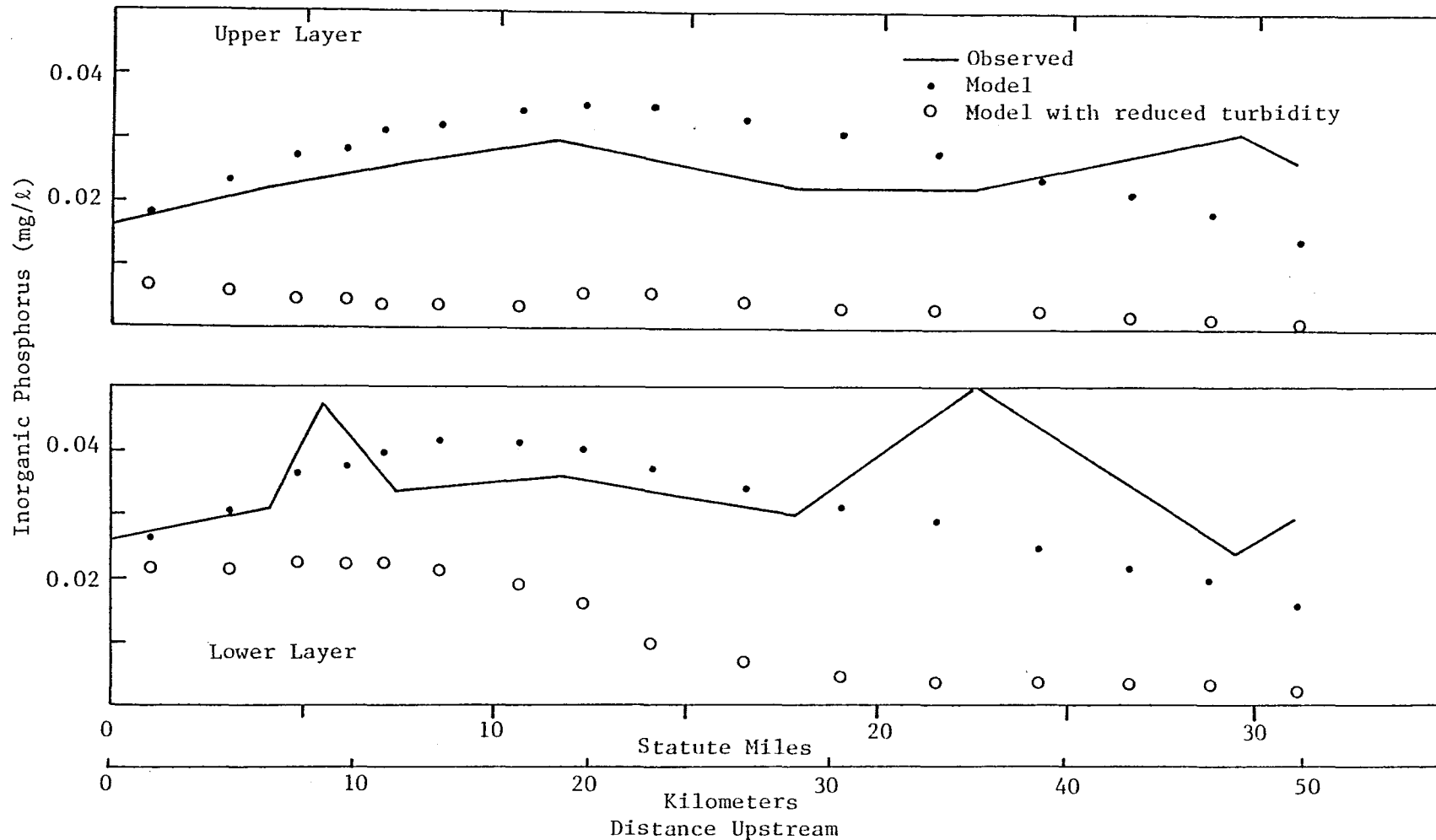


Figure 22. York River inorganic phosphorus verification.

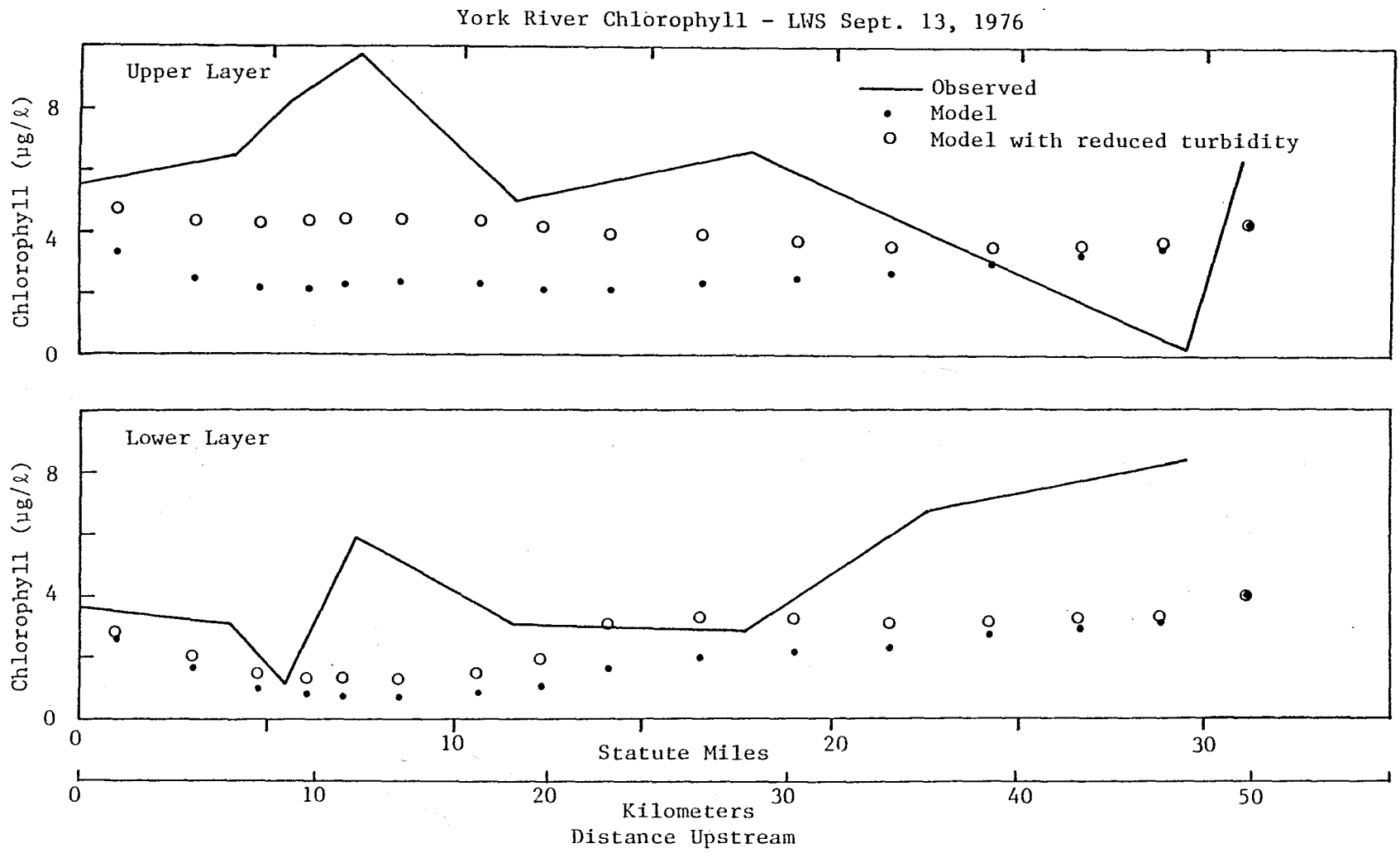


Figure 23. York River chlorophyll 'a' verification.

York River Ultimate BOD - LWS Sept. 13, 1976

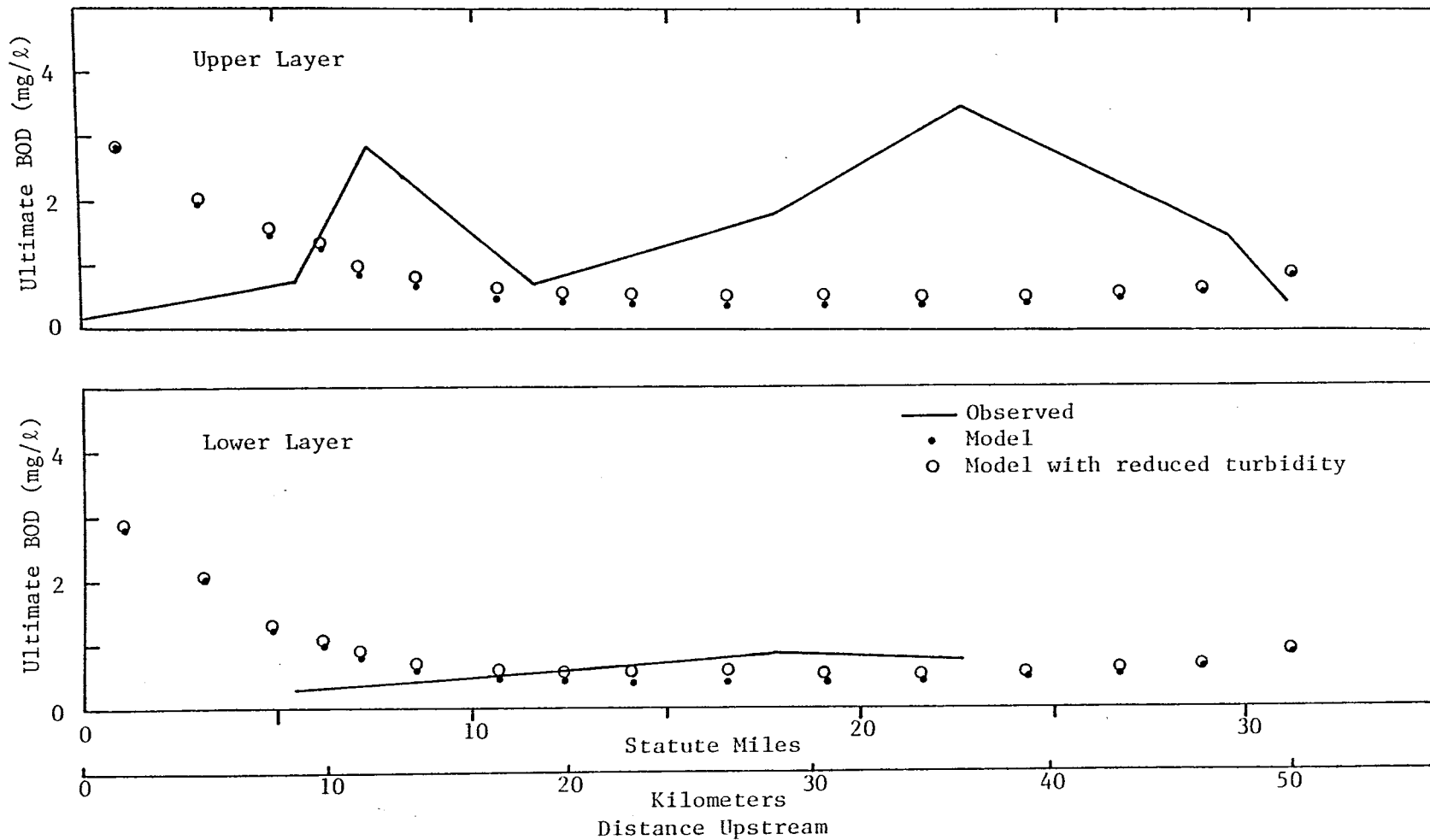


Figure 24. York River carbonaceous BOD verification.

York River Dissolved Oxygen - LWS Sept. 13, 1976

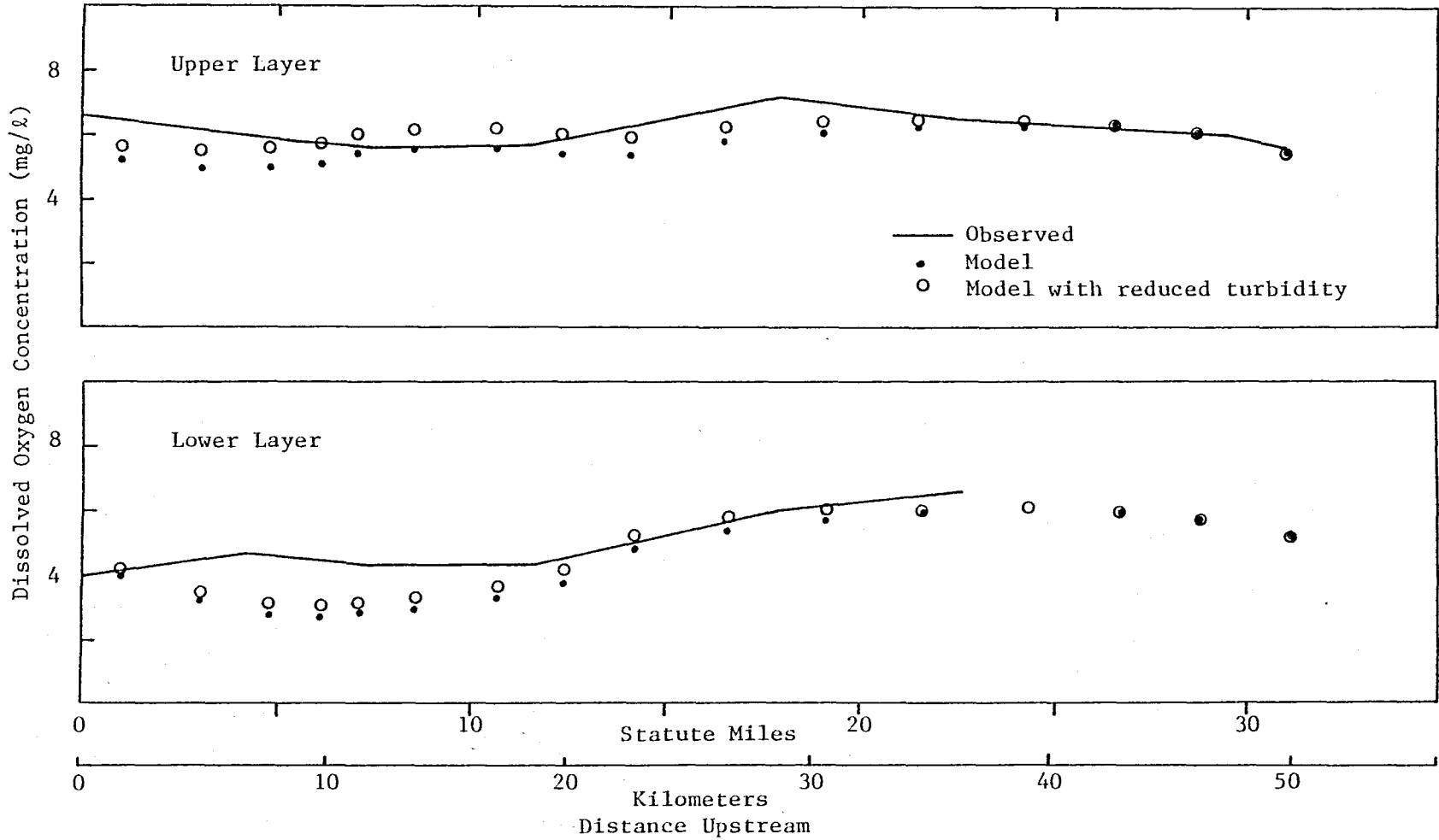


Figure 25. York River dissolved oxygen verification.

- dispersion coefficient and the constants associated with two-layer circulation, in order to clarify the role of these numbers;

- freshwater inflow and boundary conditions, since these are perforce changed between calibration and verification, so that there is a need to see just how important they are;

- certain decay constants, such as those for BOD and coliform bacteria.

Sensitivity tests were made to show the response of the model to the foregoing changes in inputs.

Figure 26 shows the carbonaceous BOD distributions that result when the point sources were either doubled or eliminated. There is little difference between the curves. This insensitivity is due to the great volume of the York River; a single reach can contain as much as 3.5×10^9 ft³. If one were to put a contaminant into this volume at a rate of 10^4 lb/day, it would take about three weeks to reach a level of one ppm, even ignoring decay and flushing.

Figure 27 shows the effect of variations in dispersion coefficient on the salinity distribution. The formula for dispersion coefficient has only one adjustable factor, β . Calibration was achieved with $\beta=2$. Figure 27 shows the salinity distribution with $\beta = 0.2$, $\beta = 2$ and $\beta = 20$. As can be seen, the salinity results are somewhat sensitive to this constant. The sensitivity of salinity to estuarine circulation vRa is shown in Figure 28. Decreasing this parameter below the calibration value had no appreciable effect, but increases in the

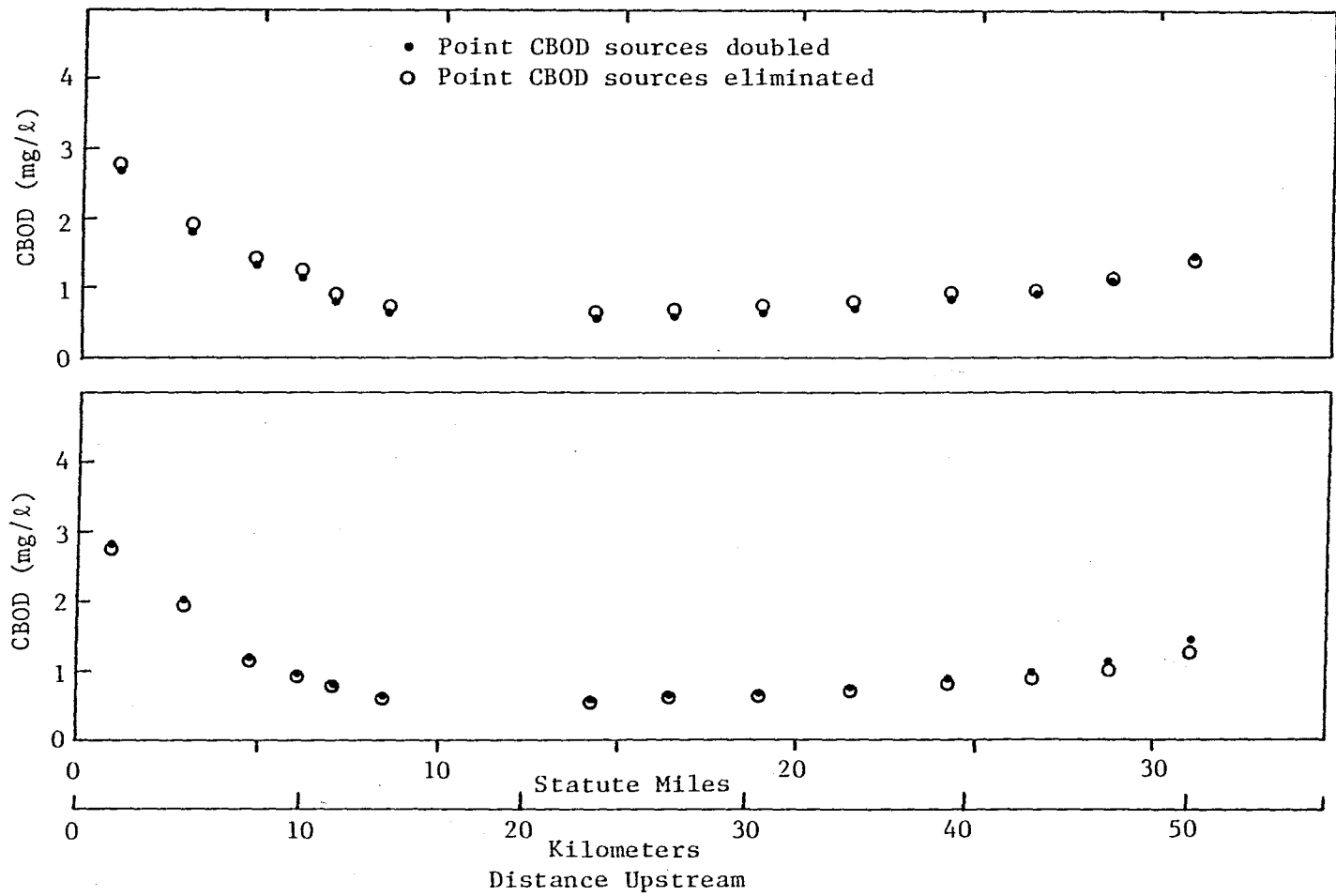


Figure 26. Sensitivity of CBOD to magnitude of point sources.

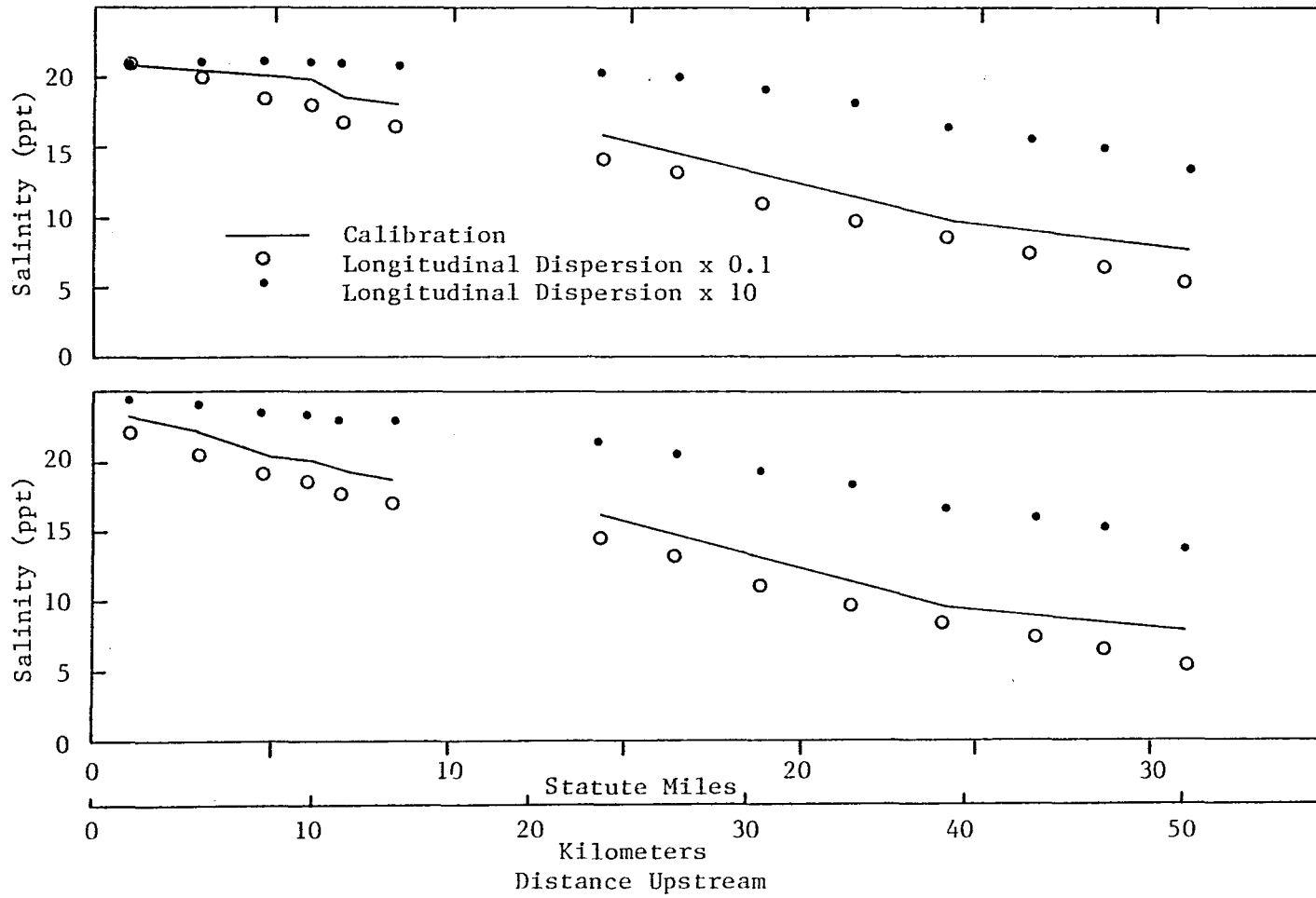


Figure 27. Sensitivity of salinity to dispersion coefficient.

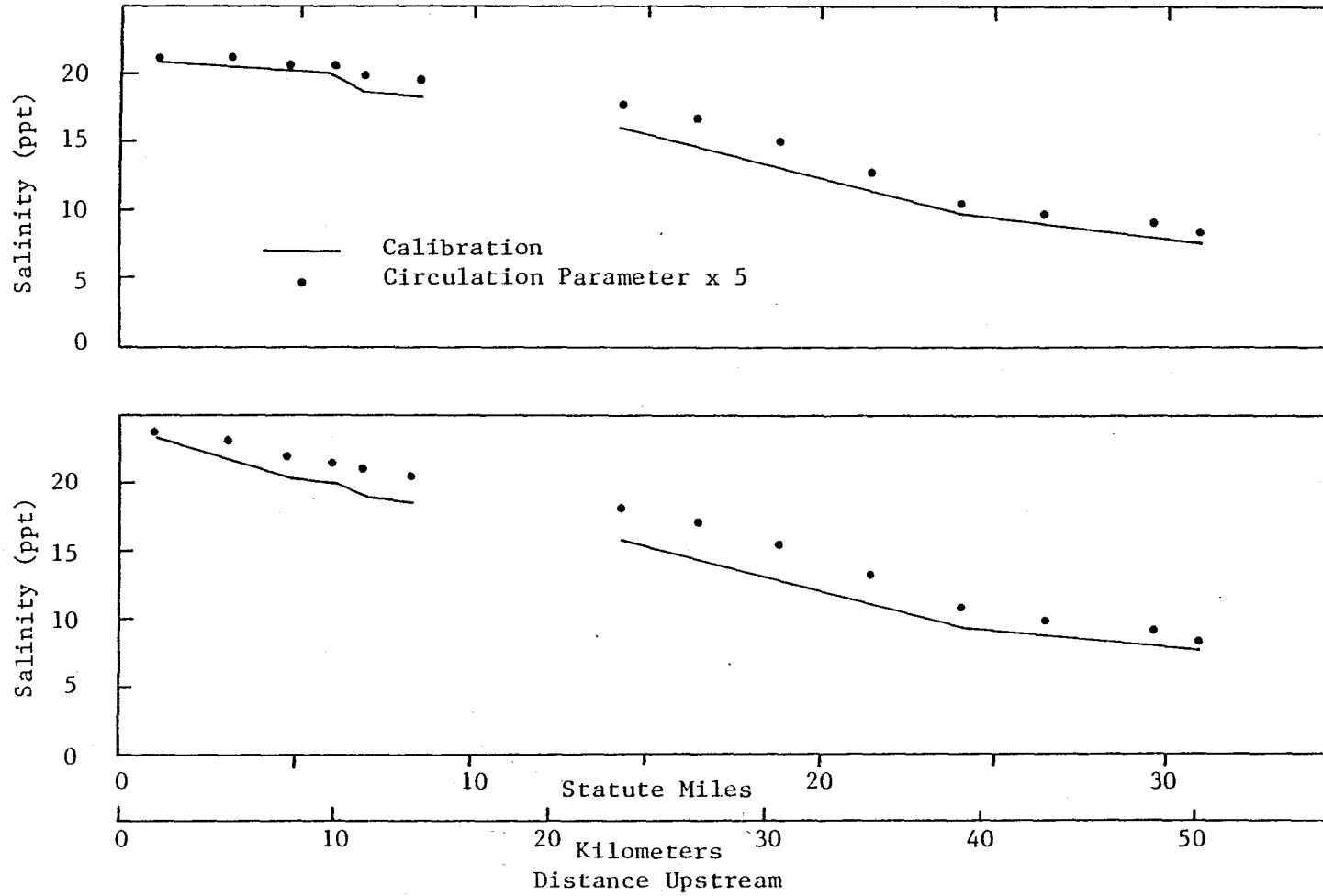


Figure 28. Sensitivity of salinity to estuarine circulation parameter.

values used did have an effect. The sensitivity of the salinity distribution to changes in the freshwater inflow is shown in Figure 29. Again the calibration value is the central number. The sensitivity of salinity to changes in the boundary conditions downstream is shown in Figure 30.

Tests were made to determine the response of the BOD distribution to changes in the BOD decay rate. These are shown in Figure 31. The same is true for the oxidation of ammonia, as shown in Figures 32 and 33. The response of fecal coliform distribution to variations in dieoff rate is shown in Figure 34.

C. Discussion

Water quality in the York River generally was quite good, with the exception of dissolved oxygen in the deep waters opposite Yorktown. In the upper layers, the daily average DO stayed above 5 mg/l except for Transect Y-2, located about five nautical miles (8 km) from the river mouth. This transect is quite close to the constriction at Gloucester Point where the channel is narrow (one kilometer or less) and very deep (about 30 meters). It is possible that water quality in this region is influenced by local dynamic effects not included in the model, such as upwelling or other secondary circulation.

Dissolved oxygen in the deep area between Gloucester Point and the river mouth was low (values as low as 2 mg/l were recorded) at the time of the intensive survey. This appears to be a naturally occurring phenomenon and not the result of

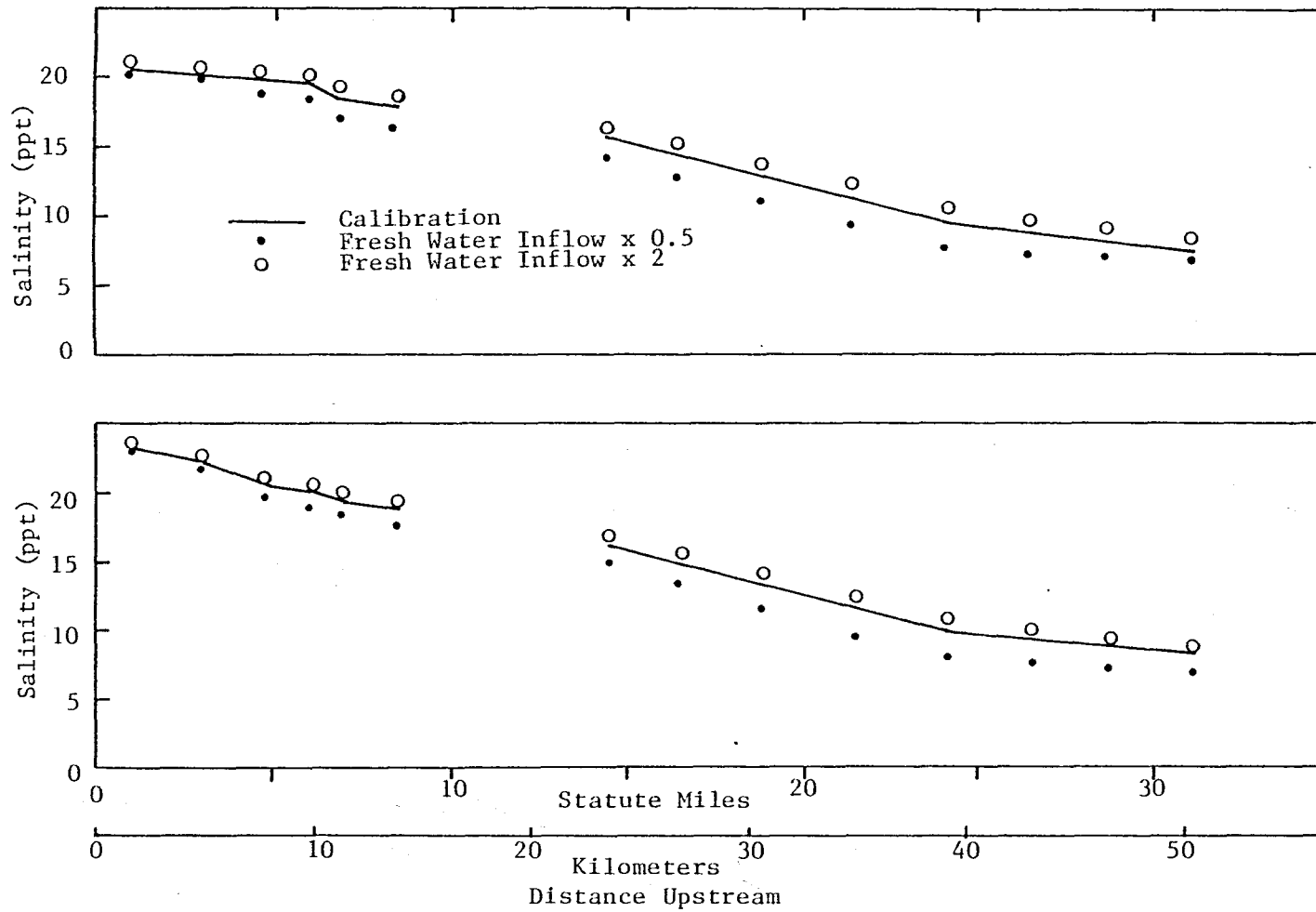


Figure 29. Sensitivity of salinity to freshwater inflow.

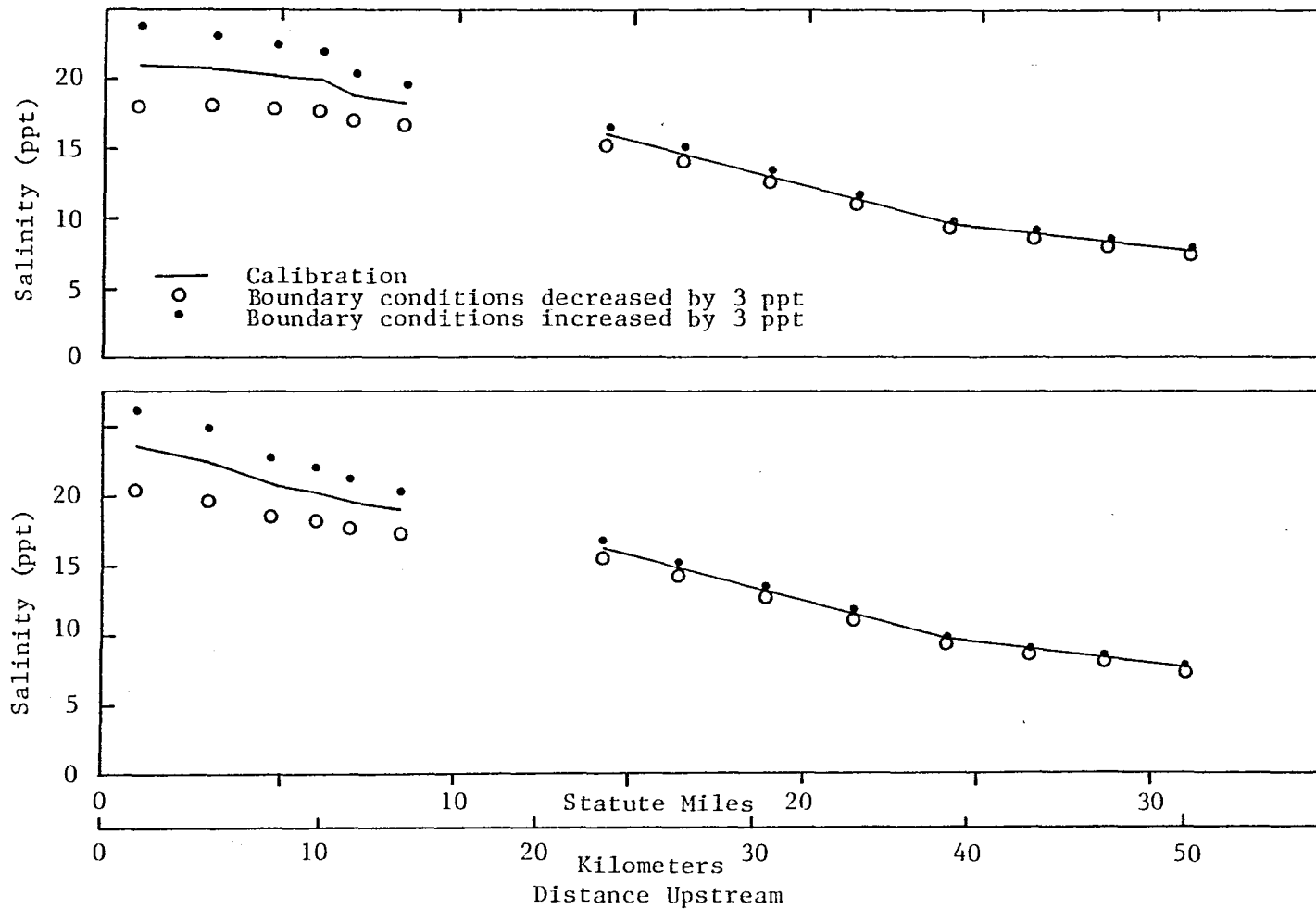


Figure 30. Sensitivity of salinity to downstream boundary condition.

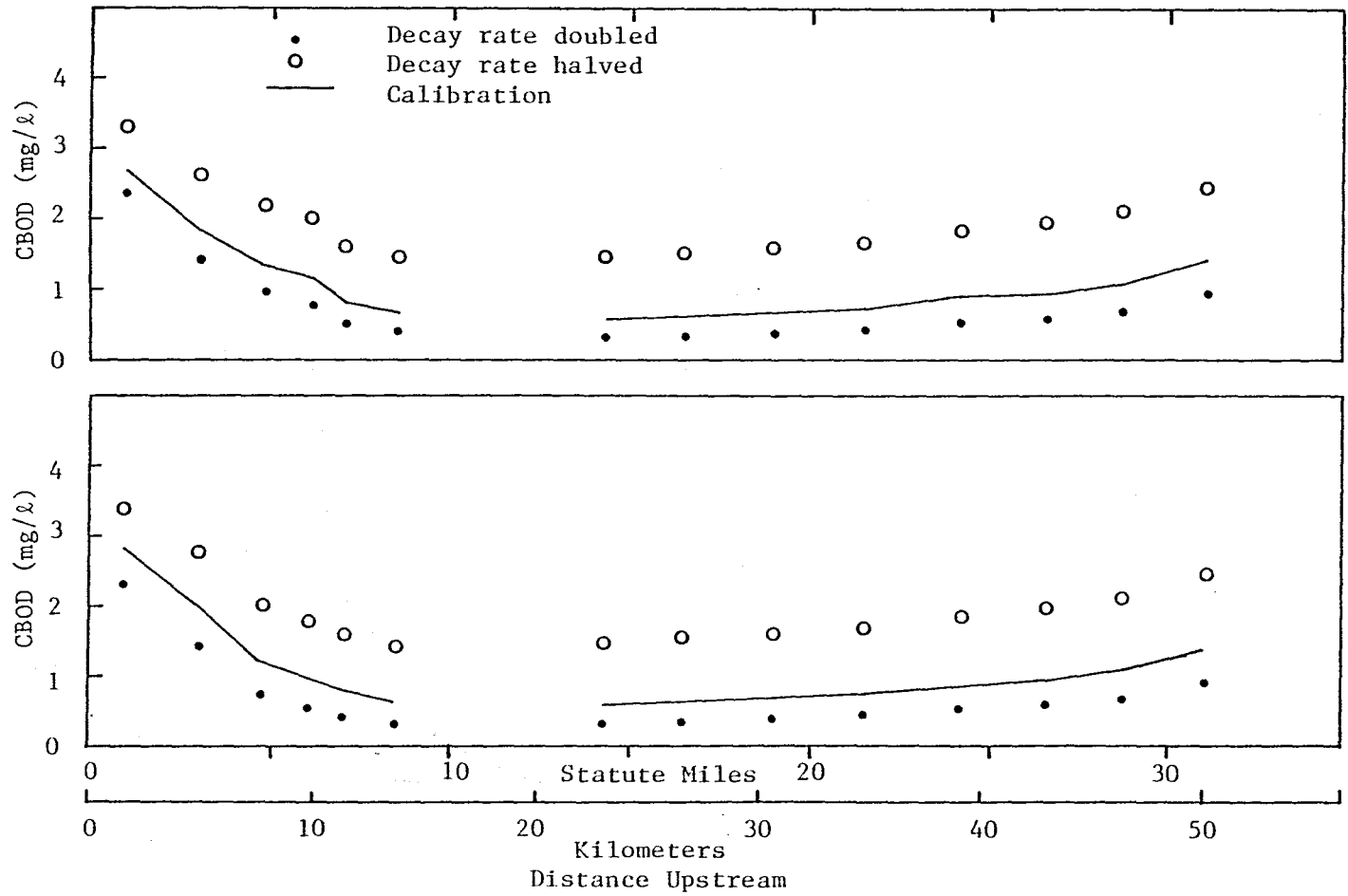


Figure 31. Sensitivity of CBOD to decay rate.

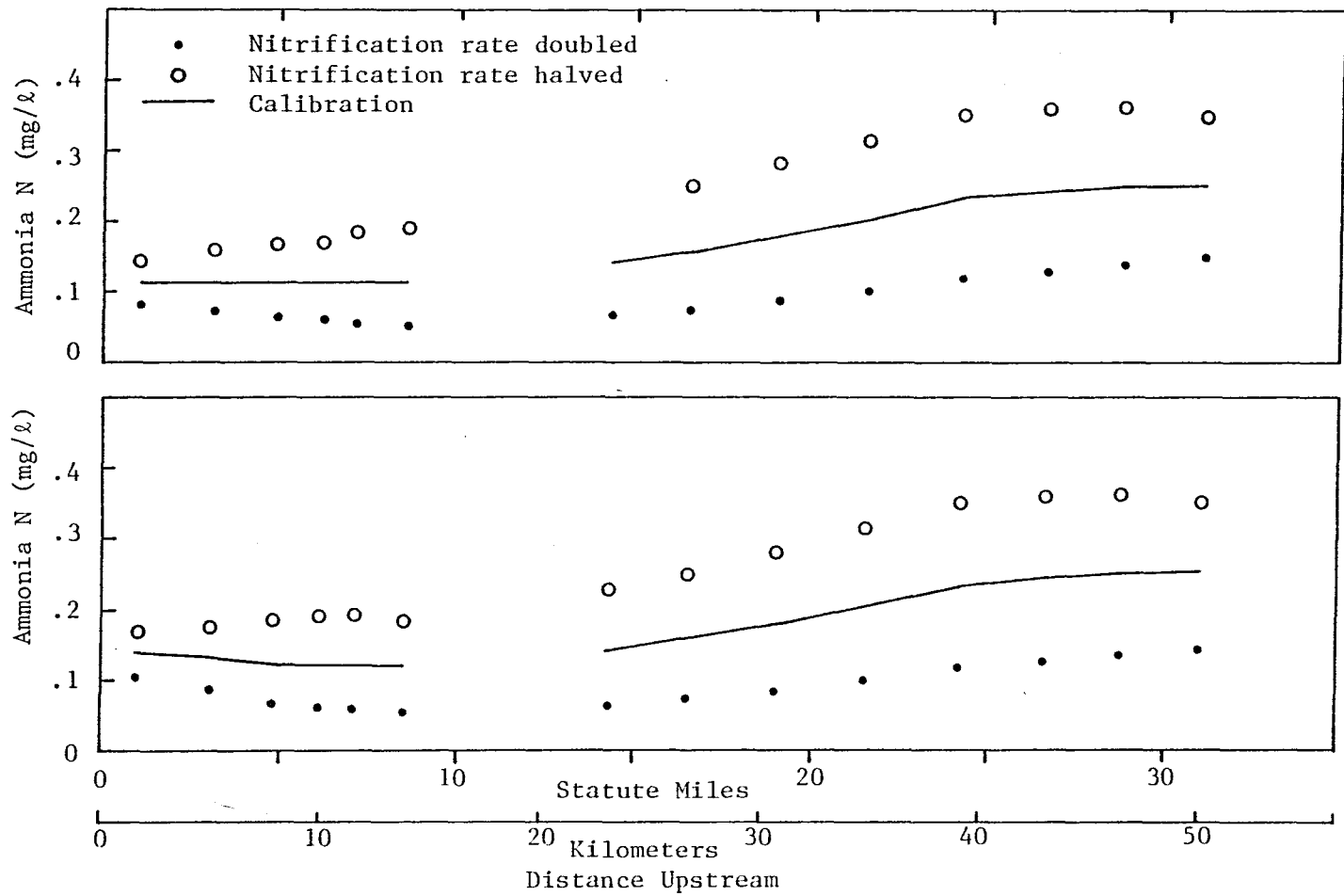


Figure 32. Sensitivity of ammonia to nitrification rate.

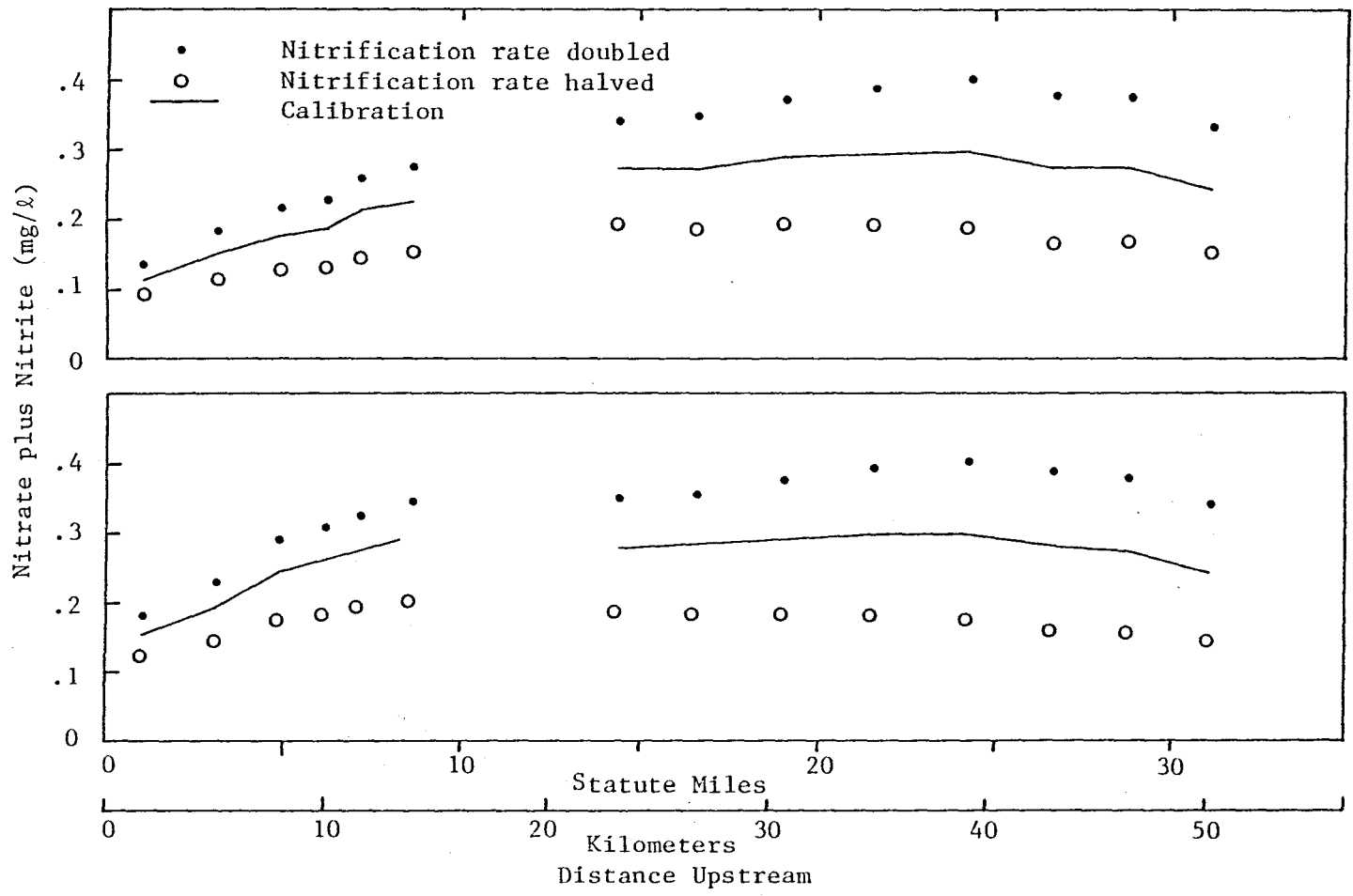


Figure 33. Sensitivity of nitrate plus nitrite to nitrification rate.

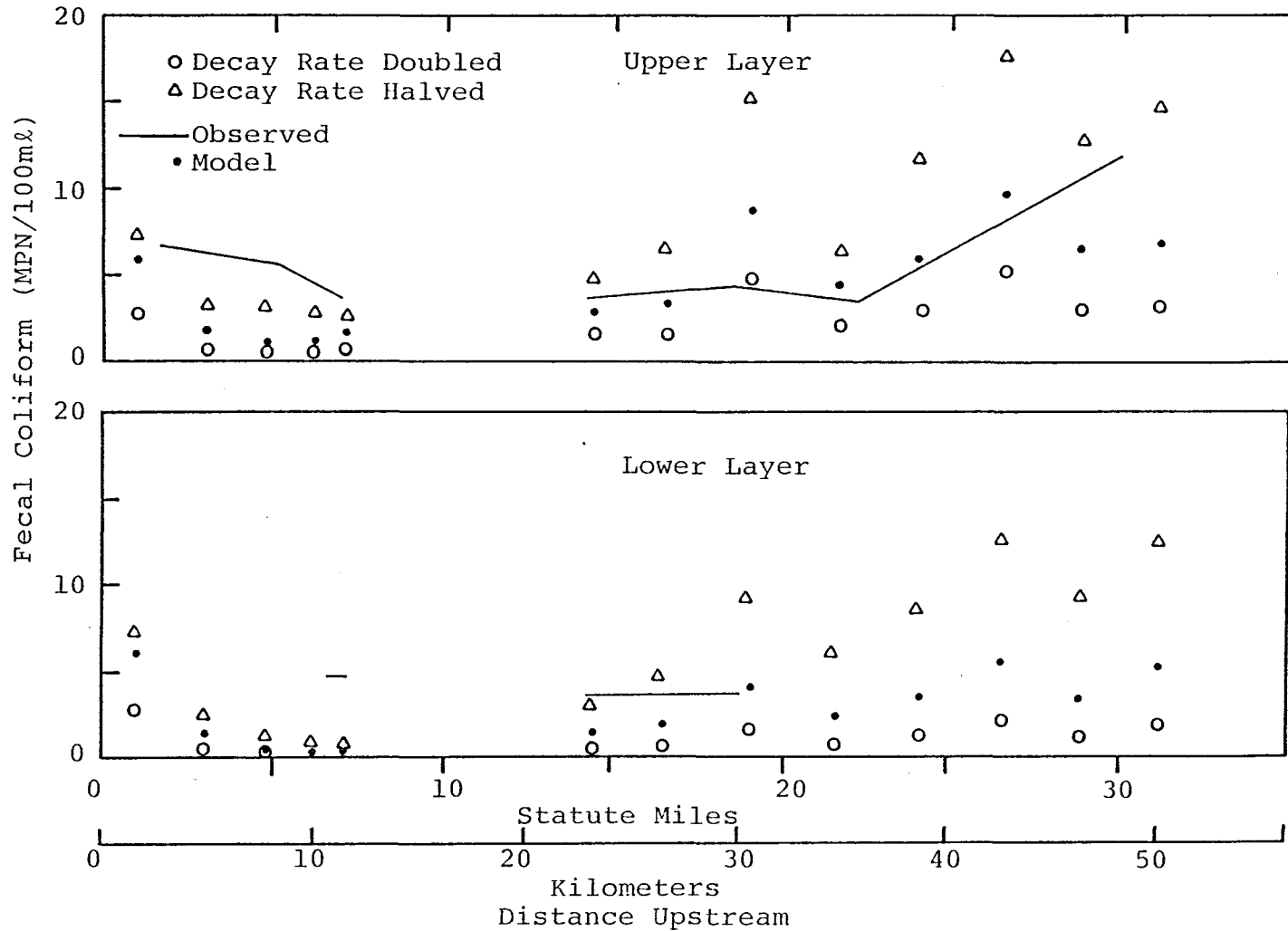


Figure 34. Sensitivity of coliform concentration to variations in bacterial decay rate.

human activities. It appears that the sill (depth around 10 meters) at the mouth of the river restricts tidal exchange and thus reduces the supply of oxygen received from Chesapeake Bay during flood tide. This relatively stagnant pool of water persists unless or until overturning takes place. Jordan's data (1975) show this condition alternately appearing and disappearing during the summer months, possibly in response to meteorological events such as extreme high tides or strong winds. The correlation between dissolved oxygen stratification and salinity stratification is not strong, suggesting that oxygen levels, once replenished, subside gradually.

The model calibration for dissolved oxygen shows very good fit but the agreement was less good for the verification run. During the slack water survey of September 13, 1976, the observed DO never went below 4 mg/l even in the deeper layer, but the model predicted DO levels below 3 mg/l. A likely cause for this discrepancy is the use of the calibration turbidity for verification in lieu of any measured value. As can be seen from the verification plots, agreement is improved considerably with a reduced turbidity. Nonetheless, the model can be considered to give reasonable, if conservative, results and to be useful for waste load allocation studies.

Observed chlorophyll "a" levels are below ten micrograms per liter and far below bloom conditions. As with dissolved oxygen, the agreement between field observations and predictions was better for the calibration than for the verification. Again the turbidity level is a major cause of this discrepancy.

Biologists also contend that the phytoplankton population will be changed in composition and identity between the beginning of July and the middle of September. Therefore, it is believed that more importance should be given to reproducing the June-July case, since these are closer to the maximum stress conditions.

Conditions observed for nutrients are consistent with those observed for chlorophyll, namely that nutrients generally are too low to support an algal bloom even if the constraint of light limitation were removed. As mentioned previously in this report, the error bars represent the standard error of the mean of the observations. Given the wide scatter of observed values, the agreement is satisfactory. Where no error bars are shown, data were insufficient to draw these. The only exceptions to this rule were fecal coliform and inorganic phosphorus. In the case of inorganic phosphorus, observed values are given only to the nearest hundredth of a milligram per liter, based on the ultimate accuracy of the laboratory method. The verification predictions show nitrite plus nitrate-nitrogen and inorganic phosphorus concentrations at higher levels than those observed in the river. This is concomittant with the low chlorophyll levels predicted and the same remarks apply. Additionally, it should be noted that the inorganic phosphorus concentrations are close to the detection limit, so that the error is small in absolute terms, even though it may appear to be large in terms of percentages.

The standard error of the mean of CBOD was large in relation to the observed mean. Agreement of the calibration was fairly good considering the uncertainties naturally inherent in this type of determination. As with nutrients, the absence of error bars indicates that the data base was too small for meaningful calculation of them. The model reproduced the general level of CBOD in both the calibration and verification runs.

The mean fecal coliform concentrations were quite close to the detection limit of 3.0 MPN/100 ml. Consequently, the observed means are biased slightly upwards by discarding observations "less than 3.0 MPN/100 ml". Furthermore, the statistical method employed in this determination introduces implicit uncertainty by giving only discrete values; there simply aren't reported values between 3.0 and 3.6, or between 3.6 and 7.3, and so forth. Error bars would therefore have little meaning even where warranted by the data base. Agreement is therefore fairly good. High coliform counts do not appear to be a problem in the York River, either now or in the future, since observed counts generally were low and there is an enormous volume of water available to dilute influent wastes.

The calibration data were collected in two field efforts separated by a period of over two weeks in which significant rainfall occurred. Since a steady load model was required it was necessary to overlook this shortcoming of the data and treat all measurements as being simultaneous. The

rate constants used were compromise values intended to achieve the best overall fit. Further field data are needed to fine-tune the model and achieve better correspondence between the model and observation.

In summary, the water quality of the York River is good, with adequate oxygen levels, low concentrations of chlorophyll 'a' and nutrients, and extremely low fecal coliform counts. The single problem was the occurrence of low dissolved oxygen concentrations in the deep waters lying between Gloucester Point and the river mouth. The water quality model has demonstrated its ability to reproduce the most critical aspects of water quality and to be useful for wasteload allocation studies.

REFERENCES

- Carritt, D. E. and E. J. Green. 1967. "New Tables for Oxygen Saturation of Seawater." *Jo. Mar. Res.*, Vol. 25, No. 2.
- Cronin, W. B. 1971. "Volumetric, Areal and Tidal Statistics of the Chesapeake Bay Estuary and its Tributaries", CBI Special Report 20, Ref. 71-2, March.
- Di Toro, D. M., D. J. O'Connor and R. V. Thomann. 1971. "A Dynamic Model of the Phytoplankton Population in the Sacramento-San Joaquin Delta." *Adventures in Chemistry Series*, No. 106, American Chemical Society, pp. 131-180.
- Elmore, H. L. and W. F. West. 1961. "Effect of Water Temperature on Stream Reaeration." *Proc. ASCE*, 87(SA6).
- Fang, C. S., et al. 1973. "Hydrography and Hydrodynamics of Virginia Estuaries. IV. Mathematical Model Studies of Water Quality in the James Estuary". Virginia Institute of Marine Science, SRAMSOE No. 41, September.
- Hansen, D. V. and M. Rattray, Jr. 1965. "Gravitational Circulation in Straits and Estuaries." *Jo. Mar. Res.* 23(2).
- Hansen, D. V. and M. Rattray, Jr. 1966. "New Dimensions in Estuary Classification." *Limnology and Oceanography*, Vol. XI(3).
- Harrison, W., et al. 1971. "Investigation of the Water Table in a Tidal Beach", Virginia Institute of Marine Science Special Scientific Report No. 60, October.
- Holley, E. R., et al. 1970. "Dispersion in Homogeneous Estuary Flow." *Jo. ASCE*, Vol. 96, No. HY8, pp. 1691-1709, August.
- Hyer, P. V., et al. 1971. "Hydrography and Hydrodynamics of Virginia Estuaries. II. Studies of the Distribution of Salinity and Dissolved Oxygen in the Upper York System". Virginia Institute of Marine Science, SRAMSOE No. 13, August.
- Hyer, P. V. & E. P. Ruzecki. 1974. "Changes in Salinity Structure of the James, York and Rappahannock Estuaries Resulting from the Effects of Tropical Storm Agnes". *Proc. Symp. on Effects of Tropical Storm Agnes*. College Park, Md., June.

- Hyer, P. V., et al. 1975. "Hydrography and Hydrodynamics of Virginia Estuaries. V. Mathematical Model Studies of Water Quality of the York River System". Virginia Institute of Marine Science SRAMSOE No. 104, October.
- Hyer, P. V., et al. 1977. "Water Quality Models of Back and Poquoson Rivers, Virginia." VIMS SRAMSOE No. 144, June.
- Jordan, R. A., et al., 1975. "Yorktown Power Station Ecological Studies, Phase II: Final Technical Report." VIMS Special Scientific Report No. 76, May.
- Kuo, A. Y. and C. S. Fang. 1972. "A Mathematical Model for Salinity Intrusion." Proc. 13th Coastal Engineering Conference, July, pp. 2275-2289.
- Thomman, R. V. 1972. Systems Analysis and Water Quality Management. Environmental Research and Applications, Inc., New York, N. Y.

APPENDIX A

User's Manual for
Quasi Three-Dimensional Ecosystem Model

- A. Inputs to Main Program
- 1a. ML - number of farthest upstream transect
 - 1b. MU - number of farthest downstream transect
 - 1c. DRAIN - drainage area upstream of transect ML
FORMAT (2I10, F10.0)
 - 2a. TMAX - upper limit of time integration by the model,
in days
 - 2b. DTT - time steps to be used in the model, in days
 - 2c. NTPRIN - number of times for which printout will be
required
FORMAT (2F10.2, I5)
 - 3a. TBD - number of hours from start of integration to 0600
 - 3b. TU - time of sunrise, in hours
 - 3c. TD - time of sunset, in hours
FORMAT (3F10.5)
 - 4. TT(I) I=1, NTPRIN - times at which computer prediction
printed out, in days
FORMAT (2F10.5)
 - 5. FC - friction coefficient
FORMAT (F10.5)
 - 6. SBG - salinity concentration in lateral inflow, in parts
per thousand
 - 7a. NIBG - organic N concentration in lateral inflow, in
milligrams per liter

- 7b. N2BG - ammonia N concentration in lateral inflow,
in milligrams per liter
- 7c. N3BG - nitrate plus nitrite N concentration in lateral
inflow, in milligrams per liter
FORMAT (3F10.5)
- 8a. PIBG - organic P concentration in lateral inflow, in
milligrams per liter
- 8b. P2BG - inorganic P concentration in lateral inflow, in
milligrams per liter
FORMAT (2F10.5)
9. CBG - chlorophyll concentration in lateral inflow, in
micrograms per liter
FORMAT (F10.5)
- 10a. CBODBG - carbonaceous BOD concentration in lateral
inflow, in milligrams per liter
- 10b. DOBG - dissolved oxygen concentration in lateral
inflow, in milligrams per liter
FORMAT (2F10.5)
11. BACBG - bacteria concentration in lateral inflow, in
number per 100 ml
12. SU - upstream salinity boundary condition array, in
parts per thousand, three lateral compartments by two
layers
FORMAT (6F10.5)
13. SD - downstream salinity boundary condition array, in
parts per thousand, three lateral compartments by two
layers
FORMAT (6F10.5)

14. NIU - upstream organic N boundary condition array, in milligrams per liter. Three lateral compartments by two layers
FORMAT (6F10.5)
15. NID - downstream organic N boundary condition array, in milligrams per liter. Three lateral compartments by two layers
FORMAT (6F10.5)
16. N2U - upstream ammonia N boundary condition array, in milligrams per liter. Three lateral compartments by two layers
FORMAT (6F10.5)
17. N2D - downstream ammonia N boundary condition array, in milligrams per liter. Three lateral compartments by two layers
FORMAT (6F10.5)
18. N3U - upstream nitrate plus nitrite N boundary condition array, in milligrams per liter. Three lateral compartments by two layers
FORMAT (6F10.5)
19. N3D - downstream nitrate plus nitrite N boundary condition array, in milligrams per liter. Three lateral compartments by two layers
FORMAT (6F10.5)
20. PIU - upstream organic P boundary condition array, in milligrams per liter. Three lateral compartments by two layers
FORMAT (6F10.5)

21. PID - downstream organic P boundary condition array, in milligrams per liter. Three lateral compartments by two layers
FORMAT (6F10.5)
22. P2U - upstream inorganic P boundary condition array, in milligrams per liter. Three lateral compartments by two layers
FORMAT (6F10.5)
23. P2D - downstream inorganic P boundary condition array, in milligrams per liter. Three lateral compartments by two layers
FORMAT (6F10.5)
24. CU - upstream chlorophyll boundary condition array, in micrograms per liter. Three lateral compartments by two layers
FORMAT (6F10.5)
25. CU - downstream chlorophyll boundary condition array, in micrograms per liter. Three lateral compartments by two layers
FORMAT (6F10.5)
26. CBODU - upstream carbonaceous BOD boundary condition array, in milligrams per liter. Three lateral compartments by two layers
FORMAT (6F10.5)

27. CBODD - downstream carbonaceous BOD boundary condition array, in milligrams per liter. Three lateral compartments by two layers.
FORMAT (6F10.5)
28. DOU - upstream dissolved oxygen boundary condition array, in milligrams per liter. Three lateral compartments by two layers
FORMAT (6F10.5)
29. DOD - downstream dissolved oxygen boundary condition array, in milligrams per liter. Three lateral compartments by two layers
FORMAT (6F10.5)
30. BACU - upstream bacteria boundary condition array, in number per 100 ml. Three lateral compartments by two layers
FORMAT (6F10.5)
31. BACD - downstream bacteria boundary condition array, in number per 100 ml. Three lateral compartments by two layers
FORMAT (6F10.5)
32. TEMP - array of water temperature for reach 1 to reach MU-1. One card per reach, containing inputs for the six compartments (3x2) in the reach.
FORMAT (6F10.5)
33. KN11, KN33, KP11, KP22 - deposition rates, in day^{-1} for organic N, nitrate plus nitrite N, organic P and inorganic P respectively.
FORMAT (4F10.5)

34. NS - number of reaches (starting with 1) for which KN12 is to be specified. Setting NS=1 causes longitudinally homogeneous input.
FORMAT (I5)
35. KN12 - array of reaction coefficients for organic N to ammonia, in units $\text{day}^{-1} \text{ } ^\circ\text{C}^{-1}$. One card per reach, containing the inputs for the six (3x2) compartments in the reach.
FORMAT (6F10.5)
36. NS - number of reaches (starting with 1) for which KN23 is to be specified. Setting NS=1 causes longitudinally homogeneous input
FORMAT (I5)
37. KN23 - array of reaction coefficients for ammonia to nitrate plus nitrite, in units $\text{day}^{-1} \text{ } ^\circ\text{C}^{-1}$. One card per reach, containing the inputs for the six (3x2) compartments in the reach.
FORMAT (6F10.5)
38. NS - number of reaches (starting with 1) for which KP12 is to be specified. Setting NS=1 causes longitudinally homogeneous input.
FORMAT (I5)
39. KP12 - array of reaction coefficients for organic P to inorganic P, in units $\text{day}^{-1} \text{ } ^\circ\text{C}^{-1}$. One card per reach, containing the inputs for the six (3x2) compartments in the reach
FORMAT (6F10.5)

- 40a. AC - carbon to chlorophyll ratio, in milligrams per microgram
- 40b. AN - nitrogen to chlorophyll ratio, in milligrams per microgram
- 40c. AP - phosphorus to chlorophyll ratio, in milligrams per microgram
- 40d. AD - oxygen to chlorophyll ratio, in milligrams per microgram
- 40e. KMN - half-saturation concentration of nitrogen for phytoplankton growth rate, in milligrams per liter
- 40f. KMP - half-saturation concentration of phosphorus for phytoplankton growth rate, in milligrams per liter
- 40g. KCG - optimum growth rate of phytoplankton, in day^{-1} .
FORMAT (7F10.5)
- 41a. RIS - saturation light level, in units of power per unit area
- 41b. RIA - average light level, in same units as RIS
- 41c. RRESP - phytoplankton death rate, in $^{\circ}\text{C}^{-1} \text{day}^{-1}$
- 41d. KCS - phytoplankton settling rate in day^{-1}
- 41e. NPREF - integer specifying which form of nitrogen is preferred as food source. If NPREF = 2, ammonia is preferred; otherwise nitrate plus nitrite is preferred
FORMAT (4F10.5, I10)
42. KGRAZ - grazing rate, in day^{-1}
FORMAT (F10.5)
43. KBAC - bacteria die-off rate, in day^{-1}
FORMAT (F10.5)

B. Inputs to subroutine HYDRAL

1. TITLE - alphanumeric information concerning the input to follow FORMAT(1X,35A2)
- 2a. NDG - the number of the data group (description of contents of individual data groups will be given below).
- 2b. NS - the number of inputs to the NDG data group.
- 2c. NAME - alphanumeric information concerning the contents of the NDG data group.

FORMAT (2I5, 30A2)

This card must be repeated at the beginning of each data group.

- a. Data Group No. 1 - geometry. In this case, NS is the total number of transects to be input. $NS > MU$ (see main program). For each transect five cards will be input, in the following order:

- al. distance, drainage area and conveyancy area.

- a. DIST(I) - distance from the mouth, in statute miles, of the I transect.
- b. ARD(I) - drainage area between the I transect and the I+1 transect.

FORMAT (6F10.5)

- a2. (ART(I,J,L), J=1,3), L=1,2 - total cross section area for the six compartments on the I transect. The three inputs for the upper layer are listed first, then the three for the lower layer

FORMAT (6F10.5)

- a3. (H1(I,J,L), J=1,3), L=1,2 - average transect depth for the six compartments on the I transect. Sequence of inputs as above.

FORMAT (6F10.5)

C. Inputs to subroutine INPUT

1. TITLE - alphanumeric information concerning the input to follow.

FORMAT (1X, 35A2)

- 2a. NDG - the number of the data groups (description of the contents of individual data groups will be given below).
- 2b. NS - the number of inputs to the NDG data group.
- 2c. NAME - alphanumeric information concerning the contents of the NDG data group.

FORMAT (2I5, 30A2)

- a. Data Group No. 1 - initial conditions. If not specified, default values are provided one value is specified for all six compartments in the same reach. If NS = 1, all reaches will be set at the specified value.
 - a1. N1 - initial values of organic nitrogen as N, in mg/l.
 - a2. N2 - initial values of ammonia as N, in mg/l.
 - a3. N3 - initial values of nitrate plus nitrite as N, in mg/l.
 - a4. P1 - initial values of organic phosphorus as P, in mg/l.
 - a5. P2 - initial value of inorganic phosphorus as N, in mg/l.
 - a6. C - initial values of chlorophyll, in micrograms per liter.
 - a7. BAC - initial values of bacteria, in number per 100 ml.
 - a8. CBOD - initial values of ultimate carbonaceous biochemical oxygen demand (CBOD) in mg/l.
 - a9. DO - initial values of dissolved oxygen, in mg/l.

FORMAT (14F5.0)

b. Data Group No. 2 - waste loads input. For each reach for which a point source of waste is to be specified, two cards are required.

bla. K - reach number

blb. J - compartment number. setting J=1 locates point source on right side facing downstream, setting J=3 locates point source on left side and setting J=2 locates point source in center.

blc. QWAST - waste-water flow rate, in cfs.

bld. WS - salinity concentration in wastewater, in parts per thousand.

ble. WN1 - organic nitrogen loading, in pounds per day.

blf. WN2 - ammonia nitrogen loading, in pounds per day.

blg. WN3 - nitrate plus nitrite loading, in pounds per day.

blh. WP1 - organic phosphorus loading, in pounds per day.

FORMAT (2I5, 6F10.2)

b2a. WP2 - inorganic phosphorus loading, in pounds per day.

b2b. WBOD - CBOD loading, in pounds per day.

b2c. DOWAST - dissolved oxygen concentration in wastewater, in mg/l.

b2d. WBAC - bacteria loading, in billions per day.

FORMAT (4F10.2)

c. Data Group No. 3 - nonpoint sources. Nonpoint source loadings specified by reach and partitioned between right side and left side by volume. Default value is zero.

c1. WN1NP(I), I=1, NS - nonpoint source loading of organic nitrogen, in pounds per day.

FORMAT (7F10.2)

c2. WN2NP(I), I=1, NS - nonpoint source loading of ammonia nitrogen, in pounds per day.

FORMAT (7F10.2)

- c3. WN3NP(I), I=1, NS - nonpoint source loading of nitrate plus nitrite nitrogen, in pounds per day.

FORMAT (7F10.2)

- c4. WP1NP(I), I=1, NS - nonpoint source loading of organic phosphorus, in pounds per day.

FORMAT (7F10.2)

- c5. WP2NP(I), I=1, NS - nonpoint source loading of inorganic phosphorus, in pounds per day.

FORMAT (7F10.2)

- c6. WBODNP(I), I=1, NS - nonpoint source loading of CBOD, in pounds per day.

FORMAT (7F10.2)

- c7. WBACNP(I), I=1, NS - nonpoint source loading of bacteria, in billions per day.

FORMAT (7F10.2)

- d. Data Group No. 4 - carbonaceous decay rate. Total of NS cards. Each card corresponds to one reach and has six inputs for the six compartments (upper layer first, then lower layer). Setting NS=1 causes all reaches to be specified the same.

- d1. (CKC(I, J, L), J=1, 3), L=1, 2 - carbonaceous decay rate, in day^{-1} .

FORMAT (6F10.2)

- d2. TCCKC - temperature correction coefficient for CBOD decay.

FORMAT (6F10.2)

- e. Data Group No. 5 - turbidity. One card of input for each of the NS reaches specified. Default value zero. Setting NS=1 causes all reaches to be specified the same.

- e1. TURB(I, J), J=1, 3 - turbidity, in m^{-1} for the three compartments in the upper layer of the I reach.

FORMAT (3F10.2)

f. Data Group No. 6 - benthic oxygen demand. One card of input for each of the NS reaches specified. Default value zero. Setting NS=1 causes all reaches to be specified the same.

f1. BEN(I,J), J=1,3 - benthic oxygen demand in gm/m²/day for the three compartments in the lower layer of the I reach.

FORMAT (3F10.2)

f2. TCBEN - temperature correction coefficient for benthic demand.

FORMAT (F10.2)

g. Data Group No. 99 - end of input. Causes exit from subroutine.